Molecularly Engineered Lectins as Anti-Influenza Agents

by

Evelyn Marie Covés-Datson

A dissertation submitted in partial fulfillment
of the requirements for the degree of
Doctor of Philosophy
(Microbiology and Immunology)
in the University of Michigan
2019

Doctoral Committee:

Professor David M. Markovitz, Co-Chair
Professor Akira Ono, Co-Chair
Professor Kathleen L. Collins
Professor Michael J. Imperiale
Professor Lori L. Isom

Evelyn M. Covés-Datson

ecovesda@umich.edu

ORCID iD: 0000-0002-9299-0878

DEDICATION

To all the people who have ever believed in me, including my teachers and mentors, my friends, and my family—especially my mom LeNelle Covés, dad Mark Datson, and husband Arun Ganesan. You power the light inside me.

ACKNOWLEDGEMENTS

I have been fortunate to call the University of Michigan home for the past twelve years and counting, first as an undergraduate student and now as an MD/PhD student. This university has empowered me with so many opportunities to learn and grow, including the programs that introduced me to research: the Undergraduate Research Opportunity Program (UROP) and the Pre-MSTP Biomedical Science Research Program, now UM-SMART. I feel so grateful to be a part of this community in which I have always felt cared for and valued by the people around me—friends, advisors, professors, mentors. It has been the genuine care of others here that has lit my path and shown me on days that I did not fully believe in myself that I was worth fighting for. I am proud to be a part of this community that fosters personal growth and development through a wealth of opportunities offered (for research, travel, outreach, education) and through the warmth of personal connection. I have grown into my adulthood here, assured in myself as a person and in my future career as a physician scientist, and I know that I thrive now in part because of what the University of Michigan community has given me.

First, I would like to thank my mentor, David Markovitz, for his wonderful guidance throughout my time as a PhD student in his laboratory. He has treated me with respect as a scientist from the beginning, calling upon my ideas and listening to my thoughts in earnest even when I first started in the laboratory. This respect made a world of difference to trusting myself as a scientist. David is very generous with his time, returning drafts at lightning speed and being just a text, phone call, or in person meeting away when I cannot wait to share exciting data or when I need to work through a scientific challenge. He has redoubled in me the willingness to

ask questions and seek guidance, and has been the prime example of a researcher who collaborates as a team with others to accomplish more than any one group could do alone. I admire his intellect, his ability to think clearly about complicated scientific issues, and his fearlessness with respect to embarking on new and diverse projects in the laboratory. I am also grateful to David for his interest in me as a person, and for caring about my wellbeing both inside and outside of the laboratory. I look forward to his mentorship and friendship in the many years to come.

The Markovitz laboratory has been a great place to pursue my graduate work. Thank you in particular to Anjan Saha, Auroni Gupta, Derek Dube, Emily Gitlin, Mark Kaplan, Maureen Legendre, Nirit Mor-Vaknin, Rafael Contreras-Galindo, Steve King, and Susana Chan. You, through your comments and suggestions, helped make my science better, and made coming to the laboratory something to look forward to even on days when experiments were in a rut. Auroni and Emily were the Master of Public Health and high school students, respectively, who worked diligently to carry out some of my dissertation research with me and whom I had the real pleasure of mentoring.

My co-mentor Akira Ono has been invaluable during the course of my PhD training. He has served as a great intellectual sounding board for generating new ideas and approaches. From him I have learned to be thoughtful about interpretations and assumptions in experiments.

The rest of my thesis committee—Kathy Collins, Mike Imperiale, and Lori Isom—has continually offered thoughtful suggestions and encouragement. They helped to make my work better and deeper, for which I am immensely grateful. Thank you to all members of my committee for showing me what it means to be a rigorous scientist. I would like to extend a

special thank you to Mike, in whose laboratory I had the pleasure to rotate; I learned a great many things from Mike, including how to read scientific work with more direction and scrutiny.

Thank you to Professor Juanita Merchant, Assistant Professor Milena Saqui-Salces, and Research Assistant Professor Yifan Liu for being my first research mentors. Yifan Liu gave me my first opportunity to work in a biomedical science research laboratory through UROP. He taught me the basics of pursuing a scientific question in a laboratory setting and introduced me to many techniques, with the humorous first step of each protocol being to get comfortable. Juanita was my PI during the majority of my undergraduate research career. She served and continues to serve as a great example of what it means to be a physician scientist, and has shared with me valuable insights from her path to becoming one. It is from Juanita that I learned how to give a good scientific presentation. Now an Assistant Professor in Minnesota, Milena was a postdoctoral fellow in the Merchant laboratory from whom I learned so many things about the day-to-day pursuit of research. She made my time in the Merchant laboratory stimulating, fun, and worthwhile, and I credit her with preparing me well to pursue my PhD training. She is also a great friend.

Thank you to the Department of Microbiology & Immunology and Molecular Mechanisms of Microbiology Pathogenesis Training Program for welcoming me and supporting me as a PhD student. I am in awe of caliber of the students, postdoctoral fellows, and faculty in these two groups, and I know I have learned a great deal from my fellow trainees and from many faculty members in the Department. I am grateful to Bonnie Krey, Heidi Thompson, Mary O'Riordan, and Eric Martens from the Department; and Margaret Allen, Adam Lauring, and Vern Carruthers from the Training Program for your attention in making a wonderful training environment for me. Thank you also to Vic DiRita for stellar instruction and mentorship, and to

Beth Moore for enthusiastically teaching me virology as an undergraduate student. Thank you to Sukhmani Bedi and Allie Dupzyk for being great friends.

I must extend many thanks to the Medical Scientist Training Program (MSTP). Ellen Elkin, Justine Hein, Hilkka Ketola, Laurie Koivupalo, and Ron Koenig have been extremely warm and helpful over the years navigating the many steps towards an MD/PhD. To all of my MSTP classmates: I feel immense gratitude that I joined this particular class of the MSTP. In it, I have found my friends for life. I would especially like to thank Jennifer Sun for birthday tea, silly selfies, and always having things to tell one another even if we have already been together all day; Anjan Saha, who has been my buddy and co-conspirator in the laboratory; Amanda Wong, one of my favorite people with whom to talk science; and Kate Brieger, for study tea and lots of reading time. Your friendship has buoyed me throughout the whole of my time in the MSTP, including during graduate school.

Additional friends outside of the MSTP who have been particularly supportive during my PhD studies include Liz Spurgeon, Lauren Seale, and Margaret Love.

My husband Arun—who has talked of wearing a banana costume on the day of my defense to support me and my work on banana lectins—is just the right amount of silly and sweet. He inspires me every day with his kindness, and encourages me every single day. He is continually excited to hear about even the smallest details of my work, which helps to keep me filled with wonder about the science also. Arun has been an immense support.

Finally, I would like to wholeheartedly thank my parents LeNelle and Mark, my additional parents Rachel and Dave, and my family as a whole. It is difficult to understate how grateful I am for a lifetime of love and support. I cherish you and everything you have given me. Thank you for my dad Mark for instilling in me a curiosity about how things work, as well as a

cool confidence that things will work out. Thank you to my mom LeNelle for being the most generous person I know. It does not go unnoticed.

The work herein was supported by grants to David Markovitz from the Defense Threat Reduction Agency (HDTRA1-15-1-0067) and the University of Michigan Michigan Translational Research and Commercialization (MTRAC) Life Sciences. I was supported by training grants from the University of Michigan Medical Scientist Training Program (T32 GM07863) and the Molecular Mechanisms of Microbial Pathogenesis Training Program (T32 AI007528) from the National Institutes of Health, and by a National Research Service Award (1F31AI136615-01) from the National Institute of Allergy and Infectious Diseases.

TABLE OF CONTENTS

LIST OF TABLES

LIST OF FIGURES

ABSTRACT

Influenza viruses pose a major threat to public health worldwide, causing both seasonal epidemics, which infect millions and kill ~500,000 people annually, and pandemics, which are unpredictable and have the potential to kill millions, as was illustrated most recently in 2009 with the "swine flu" pandemic and most dramatically in 1918 with the emergence of the "Spanish flu" that resulted in fifty million deaths. There is a strong need for a new broad-spectrum anti-influenza therapeutic, as current prevention and treatment modalities, though helpful, suffer from distinct limitations and are at best only moderately effective.

Lectins (carbohydrate-binding proteins) have been regarded as potential antiviral agents as they can selectively bind to specific glycans on viral surface glycoproteins, including those present on influenza virus. However, clinical development of lectins has been stalled by their mitogenicity, which is the ability to stimulate proliferation, especially of immune cells. We previously demonstrated that the mitogenic and antiviral activities of a lectin (banana lectin, BanLec) can be separated via a single amino acid mutation, histidine to threonine at position 84 (H84T). The resulting lectin, H84T BanLec (H84T), is virtually non-mitogenic but retains broad-spectrum antiviral activity against human immunodeficiency virus (HIV), hepatitis C virus (HCV), and multiple influenza strains, including pandemic and avian.

In this work, we found that in a lethal mouse model H84T is indeed non-mitogenic, and both early and delayed therapeutic administration of H84T intraperitoneally are highly protective, as is H84T administered subcutaneously. Mechanistically, attachment, which we

anticipated to be inhibited by H84T, was only somewhat decreased by the lectin. Instead, H84T is internalized into the late endosomal/lysosomal compartment and inhibits virus-endosome fusion. These studies reveal that H84T is efficacious against influenza virus in vivo, and that the loss of mitogenicity seen previously in tissue culture is also seen in vivo, underscoring the potential utility of H84T as a new broad-spectrum anti-influenza agent.

Decreased mitogenicity in H84T was associated with disruption of pi-pi stacking between two aromatic amino acids. To examine whether we could provide further proof-of-principle of the ability to reduce mitogenicity without removing antiviral activity, we identified another lectin, Malaysian banana lectin (Malay BanLec), with similar structural features as BanLec, including pi-pi stacking, and showed that it is both mitogenic to peripheral blood mononuclear cells and potently antiviral. We therefore engineered an F84T mutation expected to disrupt pi-pi stacking, analogous to H84T. As predicted based on structural considerations, F84T Malay BanLec (F84T) was less mitogenic than Malay BanLec. However, F84T maintained strong antiviral activity and inhibited replication of HIV, influenza, Ebola, and other viruses. The F84T mutation disrupted pi-pi stacking without disrupting the overall lectin structure.

Taken together, this work highlights the possibility of reducing mitogenicity by rational engineering to unlock the therapeutic potential of antiviral lectins in general, and demonstrates that the non-mitogenic, broad-spectrum antiviral agent H84T BanLec is a candidate to move forward clinically.

Chapter 1 – Introduction

1.1 Influenza viruses as a public health problem

Influenza viruses pose a major threat to public health, causing approximately three-five million severe infections and killing approximately 250,000-500,000 people worldwide each year in seasonal epidemics (1). In certain years, however, incidence and mortality can be even higher due to the emergence of pandemic influenza virus strains. The year 2018 marked 100 years since the deadliest influenza pandemic on record, the 1918 Spanish flu (H1N1) that killed approximately 50 million people. There have been three other influenza pandemics in the last century: the Asian flu (H2N2) in 1957, the Hong Kong flu (H3N2) in 1968, and, more recently, the 2009 swine flu (H1N1pdm09) (2).

Influenza viruses are classified into four different species: A, B, C, and D. A, B, and C cause disease in humans, though type C only causes mild disease and is thus not typically clinically relevant. A and B can both cause clinically relevant moderate to severe disease and will be the focus of this work, although the incidence of A far outweighs that of B in reported cases. Influenza A is further subdivided into subtypes based on the type of two surface viral glycoproteins known as hemagglutinin (HA) and neuraminidase (NA) that are targeted by the immune response. There are 18 known types of HA and 11 of NA (3) and subtypes are named according to the combination of the HA and NA antigen numbers. For example, H1N1 virus contains type 1 HA and type 1 NA, whereas H3N2 contains type 3 HA and type 2 NA. Influenza

B viruses are less antigenically diverse than influenza A viruses and are divided not into subtypes but into two lineages: Yamagata and Victoria (4). Only three subtypes of influenza virus have caused pandemics in humans: H1N1, H2N2, and H3N2. Influenza B viruses have never become pandemic. Following their emergence as new pandemic subtypes, these strains have historically become one of the co-circulating seasonal influenza virus strains until they are replaced by a new pandemic virus. Currently co-circulating seasonal viruses are influenza A subtypes H3N2 and H1N1pdm09, and influenza B viruses of both lineages. Other subtypes of influenza A have not acquired the ability to be transmitted widely from human to human, but have nonetheless caused sporadic outbreaks and sometimes highly pathogenic disease in human populations, including H5N1 and H7N9, transmitted from poultry to human by close contact (5).

Following historical evidence and given that the mechanism by which pandemic viruses develop is well understood (described below in "Influenza virus biology"), public health officials and influenza virus experts believe that the emergence of another pandemic influenza A virus is virtually inevitable (5, 6). The nature of pandemic influenza viruses is that they are extremely difficult to prepare for, as predicting the subtype that will emerge is nearly impossible and humans would necessarily be immunologically naïve to the virus, creating immense challenges for disease prevention and treatment. Adequate prevention and treatment of pandemic viruses requires rapid vaccine production and available therapeutic agents with activity against the newly emerged viruses. The 2009 H1N1 pandemic illustrated the difficulty in quickly producing enough vaccine to meet demand (1). A related major cause for concern for global public health is the possibility that one of the avian influenza subtypes (H5N1, H7N9, etc.) will acquire the ability to be efficiently transmitted from human to human, which would be devastating as the mortality rate in humans with those viruses can be greater than 50% (5, 6). The critical need for a

universal influenza vaccine and for broad-spectrum anti-influenza agents could not be more clear, but our current vaccines and treatments suffer from a number of limitations (see "Prevention and treatment of influenza virus disease" below).

Whether influenza virus disease is due to seasonal or pandemic virus infection, complications that contribute to morbidity and mortality include primary viral pneumonia, secondary bacterial pneumonia, myositis, myocarditis, and central nervous system disease (7). Most mortality is due either to respiratory or cardiovascular complications. Individuals over age 50, young children, pregnant women, those with chronic disease, and those who are obese are at greater risk to develop severe disease and complications.

1.2 Influenza virus biology

Influenza A and B are enveloped viruses of the *Orthomyxoviridae* family and possess a negative-sense RNA genome comprised of 8 segments (Figure 1.1A). Influenza A infects humans, pigs, birds, horses, dogs, and bats (8), whereas influenza B infects only humans and, to a lesser extent, seals (9). As described above, only influenza A has pandemic potential. This potential exists because influenza has the capacity to rapidly change via a process known as antigenic shift (10) due to its broad host range and high genetic and antigenic diversity. Certain hosts such as pigs can be infected simultaneously by two or more viruses of different host origin. When two viruses infect the same cell in this host, genomic segments can undergo reassortment to produce viruses with combinations of HA and NA antigens not previously seen by humans and to which humans are therefore nonimmune (10). Antigenic drift, which is a more gradual change of antigens, occurs in both influenza A and B and is due to the accumulation of mutations

that have a more minor phenotypic effect. Drift accounts for changes in seasonal influenza viruses and is the phenomenon that necessitates yearly updates to influenza virus vaccines (see "Prevention and treatment of influenza virus disease" below). This section describes influenza A biology unless otherwise noted.

Each genomic RNA segment is tightly complexed with multiple copies of the viral protein nucleoprotein (NP) and a single polymerase complex into units known as viral ribonucleoproteins (vRNPs). In infectious particles, all eight unique vRNPs are arranged in a 7+1 arrangement inside the particle, i.e., they are arrayed as a circle of seven vRNPs surrounding a central vRNP (11). The viral polymerase complex is comprised of the subunits polymerase acidic protein (PA), polymerase basic protein 1 (PB1), and polymerase basic protein 2 (PB2). The polymerase is responsible for both viral transcription and viral replication, as RNA-dependent RNA polymerases do not exist in host cells. The core of the particle is surrounded by the viral matrix protein M1, which is positioned in a layer beneath the viral envelope.

Hemagglutinin and neuraminidase are the two transmembrane viral surface glycoproteins that stud the host-derived envelope, along with an ion channel called M2. HA is the major surface glycoprotein, outnumbering NA by 4:1 to 10:1 depending on the virus strain (10). HA is a homotrimeric protein with a head group that contains the receptor binding site (RBS) and a stem or stalk group that contains the machinery to undergo fusion with the endosomal membrane of the target cell. The full-length monomer peptide is termed HA0, which upon activation by a cellular protease (such as the transmembrane serine proteases TMPRSS2 and TMPRSS4 (12, 13)) is cleaved into HA1 (which makes up the head) and HA2 (which, along with some residues from HA1, makes up the stem) to allow for infection to occur (14). The HA1 and HA2 subunits are linked in HA0 by a single disulfide bond. HA is heavily glycosylated with *N*-glycans (2). The

head of each monomer contains up to five antigenic sites, some of which can be masked by glycosylation. NA is homotetrameric and functions enzymatically to cleave sialic acid residues on the surface of the cell in order to promote release of the virus following budding. Like HA, it is heavily *N*-glycosylated. The viral M2 protein is also located on the surface of the cell and functions as an ion channel to transfer hydrogen ions into the viral core during the process of uncoating of the viral genome.

The stages of the influenza virus life cycle are: attachment, entry, fusion, uncoating, transcription/genome replication, translation, assembly, and budding and release, as reviewed by Bouvier and Palese (10) (Figure 1.1B). Attachment, fusion, uncoating, and assembly are most relevant to this work and so will be emphasized here. The engineered antiviral banana lectin presented in this work exerts its inhibitory effect primarily through fusion inhibition and secondarily through attachment inhibition (see Chapter 2). During attachment, HA engages sialic acid residues on the surface of the target cell through its RBS, triggering receptor-mediated endocytosis. As the endosome matures from an early to late endosome, the endosomal pH decreases and leads to a large conformational change in HA if it has been activated by proteolytic cleavage. HA changes from a more compact, "spring-loaded" structure to an elongated structure (Figure 1.2). The fusion peptide of HA in the HA2 subunit then is able to insert into the endosomal membrane. The fusion peptide is located in the N-terminus of HA2, whereas the transmembrane domain of HA2 is located in the C-terminus of HA2 (15), so insertion of the fusion peptide into the endosomal membrane bridges the endosomal membrane and the viral envelope. A further conformational change draws the two termini of HA2 closer together, bringing the two lipid bilayers closer together and allowing for a fusion pore to develop. Concomitant with acidification of HA, the M2 ion channel acidifies the viral core by

conducting protons from the endosomal lumen into the virus following the pH gradient, which prepares the virus for uncoating once the endosomal membrane and viral envelope have fused. Uncoating is the dissolution of the matrix and release of the vRNPs into the cytoplasm. Once uncoating occurs, the vRNPs are translocated to the nucleus for RNA transcription and replication of the genome. Unlike with other RNA viruses, influenza virus replication must occur in the nucleus as "cap snatching" of host pre-mRNA caps is required. Translation of viral proteins follows in the cytoplasm before assembly, budding and release. Assembly requires the coming together of particular viral proteins in a specific order; both HA and NA are involved in assembly. Release occurs as a result of the sialidase function of NA.

1.3 *N*-glycosylation and hemagglutinin

Many enveloped viruses, including influenza, contain highly glycosylated proteins. *N*-glycosylation occurs on asparagine residues at sites known as sequons with the sequence motif N-X-T/S, where X is any amino acid except proline (16). A sequon is required for deposition of the glycan, but not all sequons are necessarily *N*-glycosylated in a given protein. Sequons are thus sites of potential *N*-glycosylation, and whether a site becomes covalently linked to a glycan depends on such factors as the cell type and the physiological state of the cells. Glycan deposition also depends on the sequence of surrounding amino acids, with certain amino acids following the sequon being inhibitory to glycan deposition, and on the presence of nearby glycans that might sterically hinder deposition of another. Sequons also do not predict the type of *N*-glycan deposited. There are three types of *N*-glycans on mature glycoproteins: oligomannose (high-mannose), complex, and hybrid (16). High-mannose glycans are branched structures

terminating in mannose, complex glycans are branched structures terminating in galactose and/or *N*-acetyl-galactosamine, and hybrid glycans are a mixture of the previous two. High-mannose *N*-glycans are not common on the surface of most healthy mammalian cells (17), with the exception of healthy embryonic cells (18) and macrophages (19). However, cancer cells often exhibit abnormal glycosylation of proteins and increased expression of high-mannose *N*-glycans (20). Viruses also express a greater proportion of high-mannose *N*-glycans than do healthy human cells, raising the possibility that they could be specifically targeted by a therapeutic recognizing these glycans (see "Lectins as candidate antiviral agents" below).

N-glycosylation of proteins begins on the cytoplasmic face of the ER (16). All *N*-glycans begin with the same precursor derived from *N*-acetylglucosamine (GlcNAc). The lipid-like molecule dolichol phosphate initially receives the sugars in a stepwise manner catalyzed by transferases, ultimately producing $Glc_3Man_9GlcNAc_2$. The sugars are then transferred by oligosaccharyltransferase as an entire unit of 14 sugars to the protein. The glycans are then processed and modified as they are transported through the ER and Golgi. Early trimming of terminal glucose and mannose sugars occurs in the ER, *cis*-Golgi, and *medial*-Golgi to produce $Man_5GlcNAc_2$. In the *medial*-Golgi, this precursor is transformed into hybrid and complex type *N*-glycans. Finally, it is in the *trans*-Golgi that additional modifications are made, including modifications to the core and elongation of branches. *N*-glycans on the surface of viruses, including influenza, are derived from the host by the same processes outlined here, except that they can be processed to a lesser extent and so can be "immature," which explains why viruses often express high-mannose *N*-glycans.

Influenza HA and NA are both glycosylated and can express a mixture of all three types of *N*-glycans (2). M2 contains a single sequon, but this site has not been definitively documented

to receive a glycan (21, 22). The glycosylation pattern of HA has changed over time, e.g. an increase in the number of sequons from six to ten on the HA1 of H3 over time. As pandemic viruses evolve into seasonal strains, they often accumulate more sequons and resulting glycans, which has been proposed to shield the antigenic sites on HA from being recognized by the immune system. However, there exists a fine balance between evasion of the humoral immune response and of the innate immune lectin response, as with an increasing number of glycans, there are more opportunities for lectins to interact with HA and disrupt its activity (2). In addition, there is a potential fitness barrier to acquiring new glycans since compensatory mutations could be required to optimize function if proper functioning is reduced by glycan deposition. There are more sequons on the head of HA than on its stem (2). The sequence of the stem and the location of its glycans are more conserved than those of the head because stem glycans are critically important for proper folding and trimerization of HA, targeting it to the cell surface for assembly, and maintaining it in the metastable state required for fusogenic activity (23–25). Patterns of glycosylation on NA do change, but are not as prone to change as those on HA.

1.4 Prevention and treatment of influenza virus disease

Prevention of influenza virus disease occurs via vaccination, which must be performed yearly, as influenza viruses undergo continual and quite rapid mutational change, resulting in antigenic change in seasonal strains through antigenic drift (1, 10). That is, the seasonal strains that circulate differ enough from year to year to necessitate the formulation of new vaccine strain combinations based on strains circulating prior to February for the next year's Northern

Hemisphere influenza season and prior to September for the Southern Hemisphere season (1). The quadrivalent vaccine, which is commonly used, includes two influenza A strains (one H1N1 and one H3N2) and two influenza B strains (one from each of the two lineages, Yamagata and Victoria). Trivalent vaccines containing only one instead of two influenza B strains are also used, but quadrivalent vaccines are thought to maximize prevention. Influenza vaccines are available as inactivated and live attenuated versions and can be produced in chicken eggs or in cell culture (1). Overall, the vaccine is moderately effective, but in some years and against certain strains can have quite low effectiveness (26). For example, during the 2017-2018 influenza season, vaccine effectiveness for the circulating H3N2 strain, which represented 69% of reported infections, was only ~25% (27). Low effectiveness can occur due to the appearance of a seasonal circulating strain following formulation of the vaccine, adaptations that occur in eggs or cell culture that cause a mismatch between the vaccine strain and the circulating strain, emergence of a pandemic strain, etc. Production of a universal vaccine capable of producing immunity against all influenza virus strains is a major goal of current influenza vaccine research (28). One approach has been to develop a vaccine that elicits antibodies against the stem region of HA (29), as this is less prone to mutational change than is the head of HA.

There are three classes of drugs approved to treat influenza virus infections in the US. The adamantanes (amantadine and rimantadine), which function as M2 channel inhibitors, have been clinically obsolete since the 2005-2006 influenza season due to the emergence of extremely high levels of resistance to the drugs among circulating virus strains (30). This is often due to the S31N mutation (31), the most common adamantane resistance-conferring mutation in H3N2 and H1N1pdm09 strains, and less frequently due to V27A and L26F mutations. Adamantanes have no activity against influenza B strains since its M2 protein, BM2, is structurally different than

M2 in influenza A in that there are side chains in the channel of BM2 that obstruct the binding of adamantanes.

The neuraminidase inhibitors have activity against both influenza A and B and, until 2018, had been the only clinically available class since the 2005-2006 season. NA inhibitors (oseltamivir [Tamiflu], zanamivir, and peramivir) are moderately effective and are given to individuals with risk factors for severe disease, to hospitalized patients, and to anyone with severe disease because they decrease mortality in that setting, but they must be administered within two days of illness to have their greatest effect and may only shorten the course of the disease by 0.5-1 days. They also have a modest effect on viral shedding. The standard of care is oseltamivir. Resistance to oseltamivir has been low among globally circulating strains since the emergence of the 2009 pandemic H1N1 strain, but it can be high in certain seasons and in certain locally circulating viruses (32, 33).

In October 2018, the FDA approved the first new class of anti-influenza therapeutics since the neuraminidase inhibitors in 1999. The prototype and only member of the class is baloxavir marboxil, which interferes with the cap-dependent endonuclease protein, inhibiting the "cap-snatching" function of influenza that is required for viral replication (34). Whereas oseltamivir must be given orally twice daily for five days, baloxavir is administered as a single oral dose. The duration of symptoms is decreased by approximately the same amount by baloxavir than oseltamivir, but baloxavir appears to decrease viral load to a faster and greater extent than does oseltamivir, which may help to decrease spread of the virus. Although baloxavir has only been clinically used for a short period of time, resistance to it has already been documented to it in a few cases (35), underscoring that new antiviral drugs should continue to be developed.

There are a variety of new influenza drugs on the horizon, including some licensed in other countries such as favipiravir (a nucleoside analog RDRP inhibitor licensed in Japan to treat influenza and other RNA virus infections) (36) and arbidol (a fusion inhibitor licensed in China and Russia to treat influenza) (37), and others currently undergoing clinical trials (38).

1.5 Lectins as candidate antiviral agents

Lectins are carbohydrate-binding proteins found in microbes, plants, and animals, both invertebrates and vertebrates. They do not modify the carbohydrates to which they bind. Lectins exhibit high specificity for the type(s) of glycan(s) with which they interact, recognizing specific monosaccharides within the glycan. Those that recognize *N*-glycans, for example, can recognize and bind to mannose, galactose, glucose, fucose, *N*-acetylglucosamine, *N*-acetylgalactosamine, and/or sialic acid. For a lectin to bind to a particular glycan, not only is the identity of the monosaccharide at the potential binding site important, but also its arrangement within the glycan; the specific internal linkages between monosaccharides within the glycan dictate whether a glycan will be recognized by a given lectin (39).

Endogenous lectins in the innate immune system of mammals provide antiviral (and antibacterial) activity through recognition and binding to pathogen glycans. Mammals possess a variety of lectins that inhibit viral infection, including lectins to which influenza virus is susceptible (40). Most mammalian lectins are C-type lectins (39), so named because they require calcium ions to function. C-type lectins can be soluble or membrane-associated and they have specificity for mannose- and galactose-containing glycans, which are common on pathogens. The family of soluble lectins that acts as a part of the innate immune system is known as the

collectins, which are C-type lectins that contain collagen (2, 41). The collectins mannose-binding lectin (MBL) and surfactant protein (SP)-D that are found in respiratory secretions bind to mannose-containing glycans on influenza virus, for example, and limit infection (41–44). MBL plays a positive role limiting other viral respiratory infections, as severe MBL deficiency is associated with lower respiratory tract infections and may make individuals more susceptible to RSV infections (45). Collectins express one or more carbohydrate recognition domains and may multimerize to increase avidity for pathogens. Other C-type lectins are membrane-associated and include macrophage mannose receptor (MMR), macrophage galactose receptor (MGR), and DC-SIGN, all of which have also been reported to play a positive role in anti-influenza innate immunity (2).

Lectins from a range of species have been identified as having the potential to act as antivirals since certain lectins can bind to viral glycans/glycoproteins, potentially blocking the interaction of these glycoproteins with the cell and thereby preventing steps in the viral life cycle, e.g. entry (39). Lectins as antivirals have the potential to be specific to viruses and not human cells as the glycans they recognize may not be present, or may be present in only low amounts, on the surface of normal human cells. For example, many viruses express high-mannose *N*-glycans, whereas most healthy human cells do not (see "N-glycosylation and hemagglutinin" above). Viruses expressing high-mannose *N*-glycans on their envelopes include influenza, HIV, MERS coronavirus, SARS coronavirus, hepatitis C virus, ebolavirus, among other viruses (2, 46, 47). Some lectins with specificity for *N*-glycans recognize high-mannose, such as the antiviral banana lectin(s) discussed in this work (see "Banana lectin and Malaysian banana lectin" below), meaning that these might be particularly well suited as potential antivirals against those viruses. Indeed, our work highlights that an engineered banana lectin with

specificity for high-mannose has robust antiviral activity both in vitro and in vivo against influenza virus infection (see "Banana lectin and Malaysian banana lectin" below, and Chapter 2).

The development of lectins as clinical antivirals has been stalled due to concerns surrounding their mitogenicity (48). Mitogenicity is the ability of a substance to induce cells, particularly immune cells, to proliferate and is mediated by the cross-linking of cellular receptors on the surface of immune cells. Lectins are thought to mediate mitogenicity through binding to immune cell receptors (49), which are glycoproteins. Mitogenicity is a major concern in a potential therapeutic agent as it could result in inflammation or other unwanted side effects, limiting the usefulness of the agent. In addition, as proteins, lectins are potentially susceptible to existing or newly developed antibodies that would limit their therapeutic efficacy (50), especially if the lectin in question is routinely encountered and ingested by humans, such as those lectins found in edible plants. Though many lectins are destroyed by the digestive system, ingested lectins do enter the bloodstream at low levels, resulting in the potential for immunity to develop against them (51–53). Our work indicates that mitogenicity can be reduced or nearly eliminated by genetically engineering lectins (see "Banana lectin and Malaysian banana lectin" below, and Chapters 2 and 3), and that pre-existing immunity against lectins, at least in the specific case of a banana lectin, does not necessarily limit therapeutic efficacy against influenza virus infection (see Chapter 2).

1.6 Banana lectin and Malaysian banana lectin

We have proof of principle with two different plant lectins, banana lectin (BanLec) and Malaysian banana lectin (Malay BanLec), that we can reduce or remove mitogenicity from specific lectins via rational engineering (see Chapters 2 and 3). This strategy may increase the likelihood of clinical application of antiviral lectins.

Plant lectins are the best studied group of lectins and are divided into groups based on their structures (54). The jacalin-related lectin (JRL) group, named after the prototypic jacalin lectin isolated from seeds of the jackfruit plant (*Artocarpus integrifolia*), is defined by the presence of the β-prism I fold, which was a novel structure for lectins at the time the jacalin crystal structure was solved (55). The β-prism I fold is composed of twelve β strands arranged into three Greek key motifs with prism-like pseudo three-fold symmetry (Figure 1.3). Each Greek key is composed of four anti-parallel β strands. In banana lectin, the first and second Greek keys contain carbohydrate binding sites (CBS), with CBS I formed by the loops at the top of the first Greek key and CBS II by the loops at the top of the second (56). One loop contains a GG motif (GG loop) and the other a GXXXD motif (ligand binding loop). CBS I and II are separated by a ligand recognition loop from the third Greek key, which is thought to mediate specificity for ligands and to participate in binding to molecules more complex than simple saccharides (57). At the time its crystal structure was solved, BanLec was found to be unique in that it was the only member of the JRL family to contain a second carbohydrate binding site (56).

The JRL family is further subdivided into two groups based on carbohydrate binding specificity: the mannose-specific jacalin-related lectins (mJRL) and the galactose-specific jacalin-related lectins. Banana lectin is a member of the mJRL group, found to have specificity

for mannose and oligosaccharides containing mannose by Koshte et al. when they first isolated BanLec from *Musa paradisiaca* in 1990 (58). BanLec isolated from *Musa acuminata* by Peumans and colleagues confirmed specificity for mannose (59). BanLec naturally occurs as a homodimer of two 15 kDa (141 amino acid) monomers held together by interactions primarily between the first faces of the prisms (56, 59). Although it forms a dimer in solution at physiological pH, it is possible that BanLec has a biologically relevant tetrameric form (60, 61). (It is worth noting that the crystal structure of the recombinant BanLec protein produced in *E. coli* is highly similar to that of the naturally occurring protein (60).)

We were the first laboratory to separate the two distinct functions of BanLec, mitogenicity and antiviral activity (60). BanLec is a T cell mitogen (58–60), meaning that it causes T cells to proliferate. Our laboratory discovered that mutating BanLec at a single amino acid position significantly reduces its mitogenicity. The mutation, H84T, based on NMR spectroscopy, crystallography, and molecular dynamics modeling data, is thought to reduce mitogenicity in H84T BanLec (H84T) as compared to wild-type (WT) BanLec by disrupting the ability of H84T to bind multiple sugars. We hypothesize that this reduced ability to participate in multivalent interactions corresponds with a reduced ability to crosslink T cell glycoproteins, leading to significantly less mitogenic activity. The H84T mutation occurs in the ligand recognition loop in the third Greek key, which is thought to modulate binding to complex glycan structures (57). In WT BanLec, tyrosine 83 and histidine 84 exhibit pi-pi stacking, which we posit serves as a rigid wall separating the two CBS that "falls" upon substitution of a threonine at position 84 (60). T84 cannot interact via pi-pi stacking with Y83 and instead is able to rotate away from CBS II where Y83 and H84 would normally face. T84 can rotate towards CBS I and interact with glycans that may bind at CBS I, creating a more open binding site at CBS I, but

making it less likely for a second glycan to bind at CBS II, thus decreasing the likelihood of the multivalent interactions that are required for mitogenicity. We were eager to recapitulate the reduction in mitogenicity in another antiviral lectin to verify that the loss of pi-pi stacking conferred the reduction, but we needed to identify another candidate lectin.

Meagher et al. identified three other lectins potentially containing a second CBS based on a BLAST sequence alignment search (56), yet in the predicted ligand recognition loop, they lacked consecutive aromatic amino acids that could undergo a pi-pi stacking interaction. Thus, we undertook another BLAST sequence analysis to identify a protein with two predicted CBS with two consecutive aromatic amino acids in the predicted ligand recognition loop capable of that interaction. We identified Malaysian banana lectin (Malay BanLec) from *Musa acuminata* ssp. *malaccensis* following those criteria. Based on sequence alignment with BanLec, we predicted that Malay BanLec would have two carbohydrate binding sites separated by a loop from the third Greek motif containing a pi-pi stacking interaction, analogous to BanLec. Like BanLec, Malay BanLec was predicted to have a tyrosine at position 83 to interact via a pi-pi stacking interaction with the adjacent aromatic amino acid, but instead of a histidine at position 84, Malay BanLec has a phenylalanine. We mutated WT Malay BanLec in a fashion similar to how we mutated WT BanLec, creating F84T Malay BanLec (F84T). F84T, like H84T as compared to WT BanLec, retains antiviral activity, but has reduced mitogenicity as compared to WT Malay BanLec (see Chapter 3).

In the chapters that follow, I present our work demonstrating that H84T BanLec is a new broad-spectrum antiviral with robust efficacy in vitro and in vivo against influenza virus (Chapter 2) and that we have been able to again separate mitogenicity and antiviral activity in a

different lectin, Malay BanLec (Chapter 3). Overall, this work highlights the exciting potential of adapting antiviral lectins for possible clinical use via rational engineering.

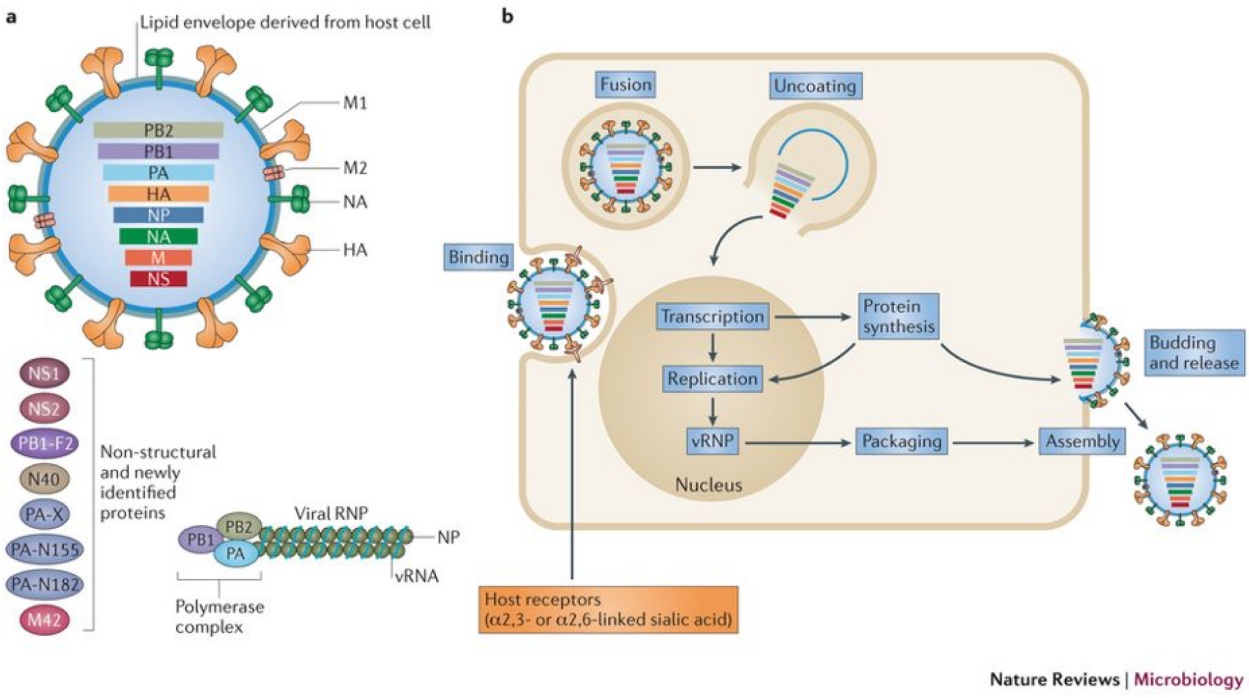

Figure 1.1 Structure and life cycle of influenza A viruses.

(**A**) Influenza A viruses are enveloped, single-stranded, negative-sense RNA viruses that contain eight gene segments that encode 16 proteins (although not all influenza viruses express all 16 proteins). The non-structural segment encodes the nuclear export protein NS2 and the host antiviral response antagonist NS1; the matrix segment encodes the matrix protein M1, the ion channel protein M2 and the M2-related protein M42 (which can functionally replace M2); the haemagglutinin (HA) segment encodes the receptor-binding glycoprotein HA; and the neuraminidase (NA) segment encodes NA (which cleaves sialic acid from cell surfaces). In addition, nucleoprotein (NP) and the components of the RNA-dependent RNA polymerase complex (PB1, PB2 and PA) are expressed from their respective genome segments. The two newly identified proteins N40 (the function of which is unknown) and PA-X, which represses cellular gene expression, are encoded by the PB1 and PA segments, respectively. Another two forms of PA (with amino-terminal truncations) have been found recently, named PA-N155 and PA-N182, which are likely to have important functions in the replication cycle of influenza A viruses. In addition, some viruses express the pro-apoptotic protein PB1-F2, which is encoded by a second ORF in the PB1 segment. (**B**) Virus infection is initiated by binding of the virus to sialylated host cell-surface receptors, and entry is mediated by endocytosis. In the host cell, fusion of viral and endosomal membranes occurs at low pH, which enables the release of the segmented viral genome into the cytoplasm. The viral genome is subsequently translocated to the nucleus, where it is transcribed and replicated. Following synthesis in the cytoplasm, viral proteins are assembled into viral ribonucleoproteins (vRNPs) in the nucleus. Export of vRNPs to the cytoplasm is mediated by M1 and NS2. Virus particles are assembled at the cell membrane, and the newly generated progeny virus buds into extracellular fluid. From Shi et al. (6).

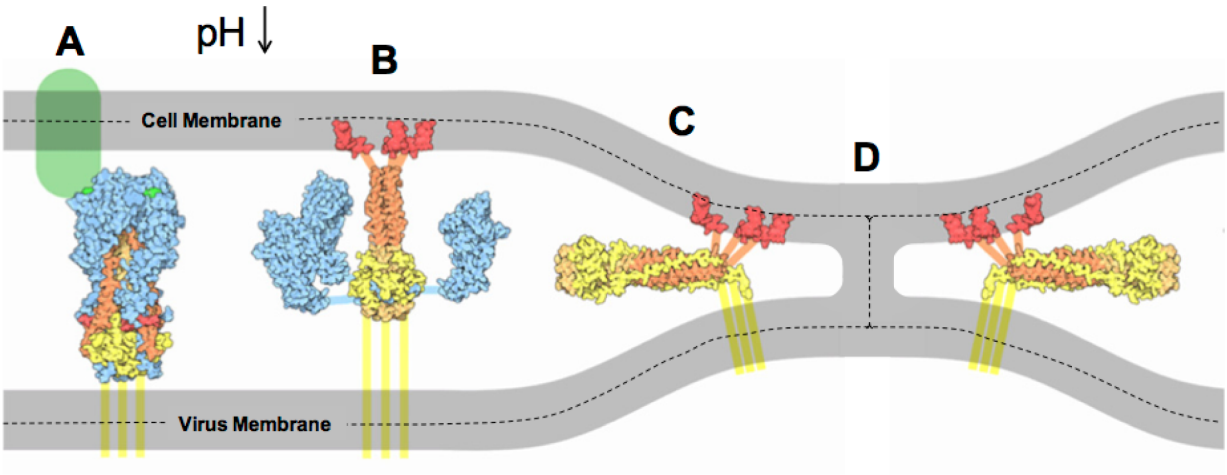

Figure 1.2 HA-mediated membrane binding and fusion between the viral and endosomal membranes.

(**A**) HA_1 (blue) binding to a moiety containing sialic acid group on the plasma membrane (light green); (**B**) After a reduction in pH in the endosome, HA_2 undergoes a conformational change that drives the fusion peptides (red) into the host cell membrane; (**C**) A further conformational change brings the outermost leaflets of the opposing membranes together to form a stalk (**D**), where it is thought to be the action of several fusogenic HA_2 working in concert. The dashed lines divide the upper and lower leaflets of the membranes for clarity. Eventually the stalk collapses to form a pore (not shown). From Hamilton, Whittaker, and Daniel (15).

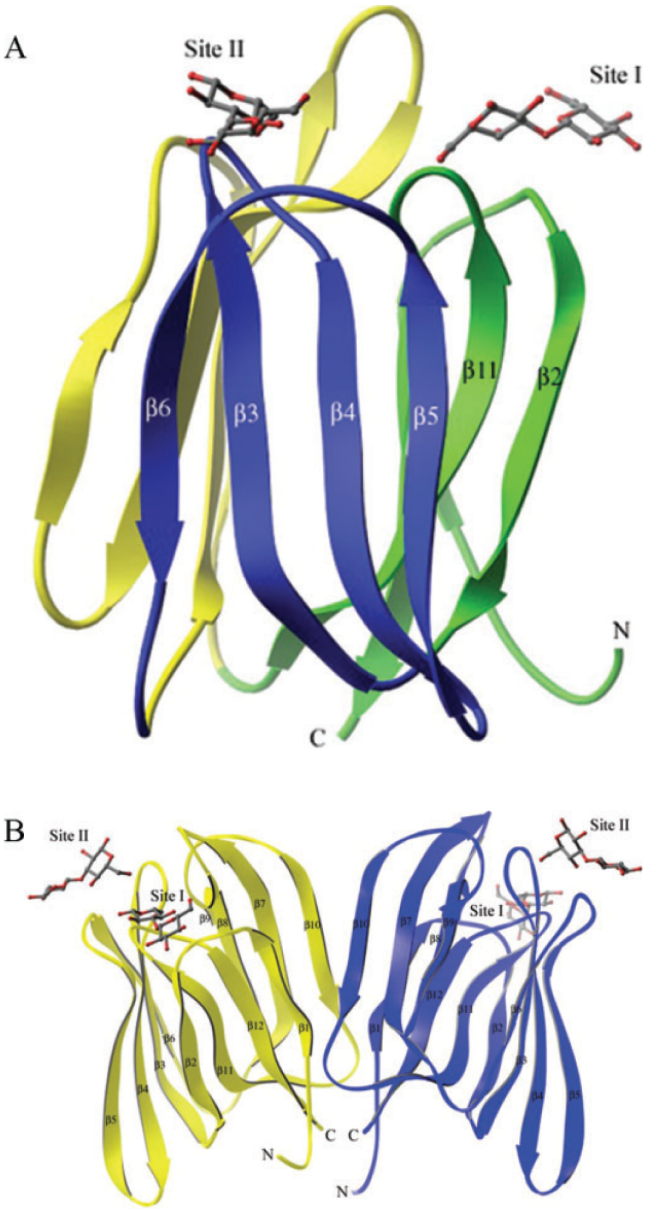

Figure 1.3 Structure of BanLec.

(**A**) Ribbon diagram of the BanLec monomer showing laminaribiose (LAM) bound in two distinct sugar binding sites. The three faces of the β-prism are colored differently, face 1 is green, face 2 is blue, and face 3 is yellow. (**B**) Ribbon diagram of the biological dimer of banana lectin (BanLec) depicting the two sugar binding sites on each monomer. In the dimer, BanLec monomers are shown in blue and yellow. In both pictures, LAM is shown in gray (C atoms) and red (O atoms). From Meagher et al. (56).

Chapter 2 – A molecularly engineered antiviral banana lectin inhibits fusion and is efficacious against influenza virus infection in vivo

This work was performed in collaboration with Steven R. King, Maureen Legendre, Auroni Gupta, Susana M. Chan, Emily Gitlin, Vikram V. Kulkarni, Jezreel Pantaléon García, Donald F. Smee, Elke Lipka, Scott E. Evans, E. Bart Tarbet, Akira Ono, and David M. Markovitz. E.M.C.-D., D.F.S., E.L., E.B.T., and D.M.M. contributed to manuscript preparation. E.M.C.-D., S.R.K., V.K., D.F.S., E.L., S.E.E., E.B.T., A.O., and D.M.M. contributed to experimental design. D.S. designed, conducted, and analyzed the in vitro combination oseltamivir-H84T studies. E.M.C.-D. and D.F.S. designed, conducted, and analyzed the in vitro efficacy studies of H84T against oseltamivir-resistant viruses. M.L. optimized production of His- and non-His-tagged H84T and His-tagged D133G BanLec and conducted the in vivo mitogenicity and distribution studies. V.V.K. and S.E.E. designed the intranasal efficacy study against H3N2 virus and V.V.K. and J.P.G. conducted it. S.M.C. and E.L. designed, conducted, and analyzed the ELISA study to determine the plasma half-life of H84T. E.B.T. designed and analyzed the IP and SC efficacy studies. E.M.C.-D., S.R.K., A.G., and E.G. conducted the in vitro mechanism of action studies. E.G. quantitated the immunofluorescence micrographs. The manuscript was submitted to *Proceedings of the National Academy of Sciences*. Comments from reviewers have been received and revisions are in progress at the time of this writing.

2.1 Abstract

There is a strong need for a new broad-spectrum anti-influenza therapeutic, as vaccination and neuraminidase inhibitors are only moderately effective. We previously engineered a lectin, H84T banana lectin (H84T), to retain broad-spectrum activity against multiple influenza strains, including pandemic and avian, while largely eliminating the potentially harmful mitogenicity of the parent compound. The amino acid mutation at position 84 from histidine to threonine minimizes the mitogenicity of the wild-type lectin while maintaining anti-influenza activity in vitro. We now report that in a lethal mouse model H84T is indeed non-mitogenic, and both early and delayed therapeutic administration of H84T intraperitoneally are highly protective, as is H84T administered subcutaneously. Mechanistically, attachment, which we anticipated to be inhibited by H84T, was only slightly decreased by the lectin. Instead, H84T is internalized into the late endosomal/lysosomal compartment and inhibits virus-endosome fusion. These studies reveal that H84T is efficacious against influenza virus in vivo, and that the loss of mitogenicity seen previously in tissue culture is also seen in vivo, underscoring the potential utility of H84T as a new broad-spectrum anti-influenza agent.

2.2 Significance statement

There is a pressing need for new anti-influenza therapeutic agents. We show that a molecularly engineered banana lectin (carbohydrate-binding protein) has broad-spectrum activity against all influenza strains tested, including drug-resistant and currently circulating strains; is safe upon repeated administration in mice; and moreover is efficacious at treating lethal

influenza infection via clinically pertinent routes of administration. We demonstrate that the lectin binds to the viral hemagglutinin glycoprotein and exerts its primary antiviral effect via inhibition of an early stage of the viral life cycle, viral membrane fusion to the host endosomal membrane. Our findings indicate that this engineered lectin, which has a mechanism of action quite distinct from the presently available agents, has potential as a new anti-influenza agent.

2.3 Introduction

Influenza viruses pose a major threat to public health worldwide, causing both seasonal epidemics, which infect millions and kill ~500,000 people annually, and pandemics, which are unpredictable and have the potential to kill millions, as was illustrated most recently in 2009 with the "swine flu" pandemic and most dramatically in 1918 with the emergence of the "Spanish flu" that resulted in fifty million deaths. Three types of influenza cause disease in humans, A, B, and C, with A and B responsible for the vast majority of the disease burden. Unfortunately, current prevention and treatment modalities, though helpful, suffer from distinct limitations and are at best only moderately effective. Vaccination must be performed yearly due to high viral mutation rates and continuous evolution of influenza antigens. Although it clearly reduces both the number and severity of cases, vaccination is often underutilized and its effectiveness varies from year to year (26). Effectiveness was estimated in the 2017-2018 US season to be only ~25% against influenza A subtype H3N2 viruses, which comprised ~69% of infections (27).

At present, although there are a number of anti-influenza agents currently in phase II or III clinical trials (38), only three classes of drugs are approved to treat influenza virus infection in the US: adamantanes, neuraminidase (NA) inhibitors, and as of October 2018, a new class

with the sole member baloxavir marboxil, a cap-dependent endonuclease protein inhibitor (34). Adamantanes are obsolete in practice due to overwhelmingly high levels of resistance to them among circulating influenza A strains and due to their intrinsic inactivity against influenza B strains. The current standard of care treatment is oseltamivir, a member of the NA inhibitor class. Oseltamivir is associated with a moderate decrease in mortality among adults hospitalized for influenza, but it must be initiated within 48 hours of illness onset to be effective and only shortens the duration of symptoms by about one day in otherwise healthy adults (62, 63). Although oseltamivir resistance among circulating strains has generally been low since the emergence of 2009 pandemic H1N1, resistance does occur and can be high in certain seasons (62, 64).

With the twin threats of another influenza pandemic and emergence of antiviral resistance ever-present and a paucity of new classes of anti-influenza drugs introduced since the NA inhibitors in 1999, there is a strong unmet need for new anti-influenza therapeutics, particularly ones that are broad-spectrum given the high genetic and antigenic diversity of influenza. Lectins, or carbohydrate binding proteins, have been proposed as potential antiviral agents due to their propensity to specifically bind the types of glycans present at high densities in glycoproteins on the surfaces of viruses. Indeed, influenza viruses are potential targets of lectins because they possess two major glycoproteins, HA and NA, which mediate key steps of the viral life cycle, including attachment to sialic acid-containing cellular receptors and fusion of the viral membrane with the endosomal membrane (HA), assembly of new virus particles (HA and NA) (65–67), and release of virus particles by cleavage of sialic acid residues (NA). However, the development of lectins for clinical use has been limited by their mitogenicity and hence potential for inflammatory side effects (48).

We have previously demonstrated that mitogenicity can be removed from a banana lectin (BanLec), while maintaining broad-spectrum antiviral activity, by engineering a single amino acid mutation at position 84 from histidine to threonine (H84T BanLec, H84T) (60). H84T is highly efficacious against pandemic, epidemic, and avian influenza in vitro and against lethal influenza virus infection in vivo when administered intranasally, yet its safety and efficacy via other clinically important routes of administration remain to be determined. In addition, though H84T is known to bind high-mannose type *N*-glycans, these glycans are abundantly present on both HA and NA (2), and thus it is not clear whether HA or NA is the key viral component antagonized by H84T. We therefore set out to determine the efficacy of systemically and subcutaneously delivered H84T, as well as the mechanism of action of H84T. Here, we report that in a lethal mouse model, H84T is indeed non-mitogenic as predicted by the in vitro data, and both early and delayed therapeutic administration of H84T intraperitoneally are highly protective, as is H84T administered subcutaneously. Mechanistically, attachment is only minorly inhibited by H84T, which was unexpected based on our observation that WT BanLec inhibits HIV attachment to cells. Instead, H84T, which can bind to HA, is internalized into the late endosomal/lysosomal compartment and inhibits the HA-mediated step of fusion with the endosome. Taken together, these studies reveal that H84T is efficacious against influenza virus in vivo, even when given up to 72 hours after challenge, and that it inhibits virus-endosome fusion, underscoring its potential use as a new broad-spectrum anti-influenza agent with a mechanism of action that is quite distinct from that of the NA inhibitors.

2.4 Results

2.4.1 H84T is active against oseltamivir-resistant and influenza B viruses and synergizes with oseltamivir in vitro

Our previous work demonstrates that H84T has robust activity against diverse influenza viruses in vitro, including A/California/04/2009 (H1N1)pdm09, A/California/07/2009 (H1N1)pdm09, A/New York/18/2009 (H1N1)pdm09, A/Perth/16/2009 (H3N2), A/Duck/MN/1525/1981 (H5N1), and the 1918 H1N1 pandemic strain, with half-maximum effective concentration (EC_{50}) values of 1-4 μg/ml (~32-128 nM) versus H1N1 virus, 0.06-0.1 μg/ml (~2-3 nM) versus H3N2 virus, and 5-11 μg/ml (~160-353 nM) versus H5N1 virus (60). Anti-influenza activity is dependent on carbohydrate binding, as the D133G BanLec mutant lacking carbohydrate-binding activity has no anti-influenza activity. Because influenza strains resistant to the standard-of-care therapy, oseltamivir, do circulate in certain years (32, 64, 68), we sought to evaluate whether H84T is effective against oseltamivir-resistant viruses. Indeed, H84T inhibited replication of A/Mississippi/3/2001-H275Y (H1N1), a strain reported to be oseltamivir-resistant (33, 69, 70), in Madin-Darby canine kidney (MDCK) cells, with an EC_{90} value of 0.074 μg/ml (2.4 nM), as compared to >100 μg/ml for oseltamivir. H84T treatment also decreased spreading infection of two other oseltamivir-resistant viruses in tissue culture, A/Texas/12/2007 (H3N2) and A/Louisiana/08/2013 (H1N1)pdm09 (Figure 2.1), in which NA inhibitor resistance is conferred by the E119V and H275Y mutations, respectively, and adamantane resistance conferred by the S31N mutation (30, 71). Thus, H84T is highly effective even against oseltamivir- and adamantane-resistant strains.

As combination therapy with both oseltamivir and H84T could be a potential strategy to treat oseltamivir-susceptible strains, we sought to determine whether synergy exists between oseltamivir and H84T. Treatment of MDCK cells infected with A/California/07/2009 (H1N1)pdm09, A/Perth/16/2009 (H3N2), A/Duck/MN/1525/1981 (H5N1), and B/Brisbane/60/2008 with both oseltamivir and H84T resulted in a virus yield reduction that exceeded one $\log_{10}$ when compared to either individual drug alone, identifying possible synergy between oseltamivir and H84T for all four viruses tested (72) (Tables 2.1-4). We further examined the effect of the drug combination using three-dimensional analysis (MacSynergy™ II) (73) and found that the combination of oseltamivir and H84T has minor but significant synergy against both A/California/07/2009 (H1N1)pdm09 and A/Perth/16/2009 (H3N2) (Figures 2.2-2.3). Thus, H84T shows some, but not striking, synergy with oseltamivir.

Since influenza B infections cannot be distinguished clinically from influenza A infections (74), anti-influenza agents that have activity against both influenza A and B are particularly attractive for empiric treatment of influenza-like illnesses. We therefore sought to evaluate whether H84T is efficacious against influenza B virus infection. We found that H84T has an IC_{50} concentration of 3-140 nM against influenza B viruses B/Brisbane/60/2008 (Victoria lineage) and B/Florida/4/2006 (Yamagata lineage) and reduces spreading infection of B/Brisbane/60/2008 in MDCK cells (Figure 2.4 and data not shown), indicating that H84T is indeed active against influenza B viruses and has promise as an anti-influenza A and B agent.

2.4.2 Intranasal administration of H84T protects against lethal H3N2 influenza virus infection

We previously reported that intranasal (IN) administration of H84T protects mice against otherwise lethal H1N1 influenza virus infection (60). To assess whether H84T is also efficacious against another influenza virus strain in vivo, we inoculated C57BL/6J mice via aerosol with a lethal dose of A/Hong Kong/8/1968 (H3N2) influenza virus and treated them with 0.1 mg/kg of H84T intranasally once daily for five days beginning four hours post-infection (Figure 2.5). Greater than 80% of H84T-treated mice survived otherwise lethal influenza virus infection, as compared to <10% of placebo-treated animals, extending the results of our previous study and indicating that H84T has robust activity against the two major contemporary subtypes of influenza A in vivo.

2.4.3 H84T, but not wild-type BanLec, is well-tolerated in vivo

Given that H84T is highly efficacious against influenza infection in vitro and in vivo via intranasal administration, we sought to further characterize its safety and efficacy in vivo when administered systemically. In BALB/c mice, we found that intraperitoneal (IP) administration of wild-type (WT) BanLec in two 50 mg/kg doses one month apart resulted in prolonged injection site lesions, characterized as erythematous papules up to a centimeter in size, in 60% of the mice lasting for up to 23 days post-injection (Figure 2.6A); piloerection of back hair for up to four days post-injection in all of the mice (Figure 2.6B); and reversible but notable weight loss of an average of approximately 10% of body weight (Figure 2.6C). These findings support in vivo the

in vitro finding that WT BanLec is mitogenic and give a stark description of how mitogenicity manifests in vivo. In clear contrast, IP administration of H84T was very well tolerated, resulting in no injection site lesions, no piloerection of back hair, and no weight loss upon administration of either dose, similar to administration of D133G BanLec, which in vitro lacks both mitogenicity and antiviral activity due to a mutation in the carbohydrate-binding site and so was not expected to elicit an inflammatory reaction. Thus, H84T appears to be non-mitogenic both in vitro and in vivo, in contrast to WT BanLec, which is poorly tolerated in mice, consistent with its mitogenicity in vitro.

2.4.4 H84T distributes to the lung

We next determined the pharmacokinetic profile of H84T in mice dosed intraperitoneally with 5, 15, and 50 mg/kg of the lectin in a single injection by measuring the concentration of H84T post-injection in both the plasma and lung (Figure 2.7A). H84T showed a dose-dependent increase in total drug exposure in plasma with a terminal half-life ranging from 33.5 to 238 h in plasma and from 25 to 32 h in the lung (Tables 2.5-6). Total exposure levels (AUC_{last}) of H84T in the lung, a key target organ for influenza treatment, exceed plasma levels significantly, but in a non-linear fashion, with a ~200-fold increase at 5 mg/kg, ~100-fold at 15 mg/kg, and ~30 fold at 50 mg/kg. Lower doses deliver a greater portion of H84T to the lung and might allow for minimizing systemic exposure if proven efficacious. Furthermore, H84T remains in the lung for greater than 72 h at the dose levels tested (Figure 2.7A). The long terminal half-life and prolonged presence of H84T in the lung raises the possibility that H84T could be administered as a single dose treatment, or at least be given at long intervals. In a parallel assessment of the

distribution of H84T, we found that H84T distributes to the lung, as well as the liver and spleen, but not to the brain or kidney in mice dosed intraperitoneally with 50 mg/kg of H84T (Figure 2.7B).

2.4.5 Therapeutic administration of H84T protects against lethal influenza virus infection

To assess the therapeutic potential of H84T delivered systemically, we inoculated BALB/c mice intranasally with a lethal dose of influenza and treated them with H84T delivered IP once daily (QD) for 5 days beginning 4 hours post-inoculation (Figure 2.8A). All mice treated with H84T at 5 mg/kg QD survived, as compared to <10% of placebo-treated animals. Furthermore, mice treated at 5 mg/kg QD up to 24 hours post-challenge all survived, as compared to approximately 90% treated with oseltamivir twice daily (BID) and <20% treated with PBS. Strikingly, 80% of mice were still protected when treatment began 48 or 72 hours post-challenge (Figure 2.8B). A key remaining question was whether H84T-treated mice would mount an antibody response to the therapeutic protein that would limit the efficacy of future H84T treatment (50). We found that mice do develop antibodies against H84T (Figure 2.8C), consistent with the finding that people develop antibodies to WT BanLec (75), but that even mice with anti-H84T antibodies generated at a time of prior H84T administration are 100% protected from lethal influenza infection by H84T treatment (Figure 2.8D). These mice also suffered no histological or biochemical damage to the lung, liver, spleen, blood, or other organs.

H84T confers robust anti-influenza protection when delivered intraperitoneally, but in a clinical setting intravenous administration, which is analogous to intraperitoneal administration, of H84T would likely be limited to hospitalized patients. On the other hand, subcutaneous

administration of H84T, if efficacious, would provide the important advantage of being feasible in the outpatient setting. We therefore examined whether subcutaneous administration of H84T conferred protection against lethal influenza virus infection in mice (Figure 2.8E). BALB/c mice were inoculated intranasally with a lethal dose of influenza virus and survival of the mice monitored after treatment with one or two 50 mg/kg doses of H84T. H84T provided 100% protection from challenge when administered in a two-dose regimen at 4 hours pre-infection and 4 days post-infection, as compared to <10% survival in the placebo-treated group. In addition, two doses of H84T provided 60% protection when administered at 24 hours and 96 hours (4 days) post-infection, and a single dose at 24, 48, or 72 hours provided 50% protection. Oseltamivir, used as the positive control, protected 70% of mice when administered BID for 5 days starting 48 hours post-infection.

2.4.6 H84T binds to HA specifically, but only minorly decreases attachment of influenza virus

A detailed mechanistic understanding of H84T's ability to inhibit influenza replication is key to developing it as a potential new therapeutic (76, 77). H84T is known to bind to high-mannose structures and perhaps other types of *N*-glycans such as can be found on the influenza virus glycoproteins HA and NA. To ascertain whether H84T interacts with HA, we performed enzyme-linked immunosorbent assays (ELISA) using recombinant HA from A/California/07/2009 (H1N1)pdm09 and A/Perth/16/2009 (H3N2), with the D133G BanLec mutant as a control, as it does not bind carbohydrates. We observed that H84T binds HA in a concentration-dependent manner, and HA shows much reduced binding to D133G (Figure 2.9A), which suggests that H84T

could potentially inhibit HA-mediated steps. The known H84T ligand methyl α-D-mannopyranoside was able to inhibit binding of H84T to HA in a concentration-dependent manner (Figure 2.9B). Unsurprisingly, it took a relatively large concentration of the sugar to compete for HA binding since there are predicted to be a large number of interaction sites for H84T on the HA glycans (2, 78). A higher concentration of the sugar was required to inhibit binding to H3 HA than to H1 HA. The binding to HA was specific, since galactose, known to not be a ligand for H84T (60), was not able to inhibit binding to HA (Figure 2.9C). Yeast mannan, which contains more mannose residues than does methyl α-D-mannopyranoside (79), was able to inhibit binding to HA at 10-fold lower concentrations (Figure 2.10).

HA mediates both early and late stages of the virus life cycle, including attachment and entry, fusion, and assembly, whereas NA, another potential target for H84T, primarily mediates late stages, including assembly and budding (66). To understand whether H84T exerts its primary inhibitory effect against influenza virus replication early or late in the influenza virus life cycle, we assessed whether viral protein expression was reduced by H84T. Arbidol (ARB), a viral fusion inhibitor that locks HA in a non-fusogenic conformation (37), was used as a positive control for inhibition of early stage infection. A dose-dependent reduction in viral protein expression was observed at 5 hours post-infection (hpi) with A/WSN/1933 (H1N1) (Figure 2.11A and B), suggesting that H84T inhibits a step at or before viral protein translation. Inhibition was dependent on carbohydrate binding, as D133G did not block viral protein expression. H84T also inhibited a step at or before protein translation 5 hpi with a virus pseudotyped with the HA and NA of A/Colorado/15/2014 (H3N2), a strain representative of the 3C.2a clade of H3N2 viruses that encompassed the majority of the ~69% of clinical influenza infections caused by H3N2 strains in the 2017-2018 season, for which vaccine effectiveness was only ~25% (27) (Figure 2.11C and D).

To ensure that the decrease in viral protein expression observed could not be attributed to toxicity, we measured cytotoxicity of H84T on MDCK cells. At 24 hours post-treatment, there was no decrease in cell viability at the IC_{50} concentration for H1N1 virus (~1-140 nM), and minimal decreases above it, suggesting that cytotoxicity could not account for the observed decrease in viral protein expression (Figure 2.12).

We next sought to further delineate the step at which H84T inhibits influenza virus replication, hypothesizing that H84T would inhibit influenza virus at the attachment or fusion steps, since we previously found that those (especially the former) are the steps at which WT BanLec inhibits HIV infection (78). To investigate whether attachment was decreased by H84T, we infected MDCK cells for 1 h at 4ºC with A/WSN/1933 (H1N1) that had been pre-incubated for 30 min with concentrations of H84T from 1-10,000 nM, the timing and temperature allowing the virus only to attach but not progress to post-attachment steps. After washing cells to remove excess virus, we collected the cells and extracted whole-cell RNA. We then measured the amount of cell-associated virus, which represents the amount of virus that has undergone attachment, by qRT-PCR. We observed that cells infected with virus that had been pre-incubated with H84T showed a minor decrease in the amount of cell-associated virus, to a much lesser extent than did cells infected with virus that had been pre-incubated with the monoclonal antibody H17-L19, known to inhibit attachment of this strain (80) (Figure 2.13A). In parallel, H84T also could not inhibit hemagglutination of turkey red blood cells (RBCs), which depends on interactions between HA and RBCs that are akin to those between HA and the cell during attachment, by the virus (Figure 2.13B). These results suggest that attachment is only minorly inhibited by H84T, which was surprising as this was the step at which HIV was predominantly inhibited by WT BanLec (78).

2.4.7 H84T inhibits endosomal fusion of influenza virus

Given that inhibition of attachment does not appear to be the major mechanism of action of H84T, we next investigated whether fusion is decreased by H84T (Figure 2.14). Dequenching of the fluorescent membrane probe R18 from R18-labeled virus was measured in MDCK cells pre-treated with the fusion inhibitor ARB, as a positive control, or H84T. When incorporated into the viral membrane at a high molarity, R18 quenches itself, but when fusion of the viral membrane with the plasma membrane is induced by a low pH fusion buffer, R18 diffuses laterally across the much larger plasma membrane, becoming dequenched and fluorescing (81–83). Triton X-100, as a detergent, induces maximal dequenching and the highest fluorescence of R18. Labeled virus was allowed to attach to cells in the presence of ARB or H84T before the addition of fusion buffer, after which fluorescence dequenching was measured. In cells incubated with virus, fusion buffer alone increased fluorescence to levels near to those from Triton X-100-treated cells, indicating that fusion with the plasma membrane had occurred. Treatment with 40 μM ARB or 1 and 10 μM H84T significantly reduced fluorescence dequenching upon exposure to low pH, which suggests that H84T may act by inhibiting viral fusion.

If fusion of influenza virus is inhibited by H84T, we reasoned that the next step in the virus life cycle would also be inhibited, namely uncoating of the viral ribonucleoproteins (vRNPs). With uncoating, the viral matrix protein (M1), which forms the scaffolding between the viral membrane and the vRNPs, dissociates from its pre-fusion location beneath the membrane and disperses throughout the cytoplasm of the cell. Detection of diffuse M1 by immunocytochemistry has thus been used at early infection time points (2.5 hours, before protein translation leads to the production of more M1) to determine in which cells uncoating, and thus

fusion immediately before it, has occurred (84). After 2.5 hours of infection with A/WSN/1933 (MOI 0.5), many MDCK cells displayed diffuse cytoplasmic staining of M1, indicating that uncoating had occurred in these cells (Figure 2.15A and B). As expected, the number of cells with diffuse M1 staining was significantly decreased by treatment with ARB. H84T also reduced the number of cells with diffuse M1 staining in a dose-responsive manner, indicating that H84T prevents events (such as fusion) that occur before (or at) uncoating of the virus (Figure 2.15C). Instead of diffuse M1 staining, virtually all of the ARB-treated infected cells and increasing numbers of infected cells treated with H84T in a dose-dependent manner exhibited perinuclear, punctate staining of M1 (Figure 2.15B), consistent with localization in the late endosome. The reduction in diffuse staining of M1 was observed both when the cells were pre-treated with H84T and when only the virus was pre-treated with H84T, suggesting that pre-conditioning of cells is not required for H84T to exert its anti-influenza activity (data not shown). We performed these studies with two more recently circulating strains, A/Florida/3/2006 (H1N1) and A/Perth/16/2009 (H3N2), and again observed the same decrease in diffuse M1 staining and increase in perinuclear punctate M1 staining with H84T treatment (Figure 2.16). These results suggest that H84T prevents exit of influenza viruses from the endosome. Indeed, co-localization between M1 in the M1-positive punctae and the late endosomal/lysosomal marker LAMP1 is high in H84T-treated cells as compared to untreated infected cells (Figure 2.17). These results indicate that uncoating is inhibited by H84T, consistent with a block at the step of fusion and restriction of the virus to the endosome.

2.4.8 H84T is internalized into the late endosomal/lysosomal compartment

Because H84T inhibits fusion between the virus and the endosomal membrane, we hypothesized that it might be internalized into the endosome in infected cells, but not in uninfected cells, via binding to hemagglutinin. However, interestingly, H84T treatment alone increases the size of LAMP1-positive punctae in cells relative to untreated cells (Figure 2.18), suggesting that H84T may be internalized even in the absence of virus, as has been demonstrated for other lectins (85, 86). As predicted, immunofluorescent staining for BanLec revealed that H84T is internalized into punctae that resemble late endosomes/lysosomes (Figure 2.19) in both infected and uninfected cells; D133G is internalized into cells to a dramatically lesser extent. To examine whether H84T is internalized into the late endosomal/lysosomal compartment in the absence of influenza virus infection, we next treated cells with His-tagged H84T or D133G and performed immunofluorescent staining for the His tag and LAMP1. Co-localization between the His tag and LAMP1 was high in H84T-treated cells (Figure 2.20), indicating that H84T localizes to the late endosome/lysosome, whereas D133G-treated cells exhibited minimal His tag staining, consistent with the low degree of BanLec staining in D133G-treated cells (Figure 2.19). In rare D133G-treated cells, His tag staining resembled that in H84T-treated cells and co-localization between the His tag and LAMP1 was high (Figure 2.20, inset), suggesting that in the rare cases that D133G is internalized, it localizes to the same compartment as does H84T. Given that both M1 and LAMP1, as well as H84T and LAMP1, colocalize to a high degree in H84T-treated cells, it is likely that H84T and the virus also colocalize in the late endosomal/lysosomal compartment, ideally positioning H84T for inhibition of fusion.

2.5 Discussion

That influenza viruses continue to cause an enormous burden of disease, morbidity, and mortality worldwide is indicative of the inadequacy of current prophylactic and therapeutic anti-influenza interventions. There has been much interest in recent years in engineering a universal vaccine or therapeutic antibody that is capable of offering protection against both influenza A and B viruses, but presently vaccines must still be given seasonally and efficacy hovers around 50% overall in some studies (26), being yet lower in certain years and against certain strains. With only a sole class of anti-influenza agents available for influenza virus treatment in the US, the NA inhibitors, until very recently (34), there has also been considerable effort to develop and approve new treatments, thus far without much success. In the event of the emergence of another pandemic influenza, believed to be an inevitability rather than a probability, effective, broad-spectrum treatment as well as vaccination would have to be deployed rapidly, necessitating the development of new anti-influenza agents capable of targeting a wide range of strains.

In this and our previous work, we have demonstrated that an engineered banana lectin, H84T BanLec, is highly active against an array of influenza virus strains. It is particularly striking how broad-spectrum H84T proves to be, capable of inhibiting multiple oseltamivir-resistant as well all other influenza virus strains tested in this and our previous study; H84T inhibits both influenza A and B type viruses and a representative of the currently circulating 3C.2a clade of H3N2 viruses, which has proven especially deadly in the 2017-2018 Northern Hemisphere influenza season (27). The finding that there is some synergy between H84T and oseltamivir raises the possibility of combination therapy, which might be more effective than single agents alone and limit the development of resistance. Influenza B, owing to its less

genetically and antigenically diverse HA and NA antigens, does not possess the pandemic potential of influenza A, but it contributes significantly to the morbidity and mortality of seasonal influenza, and thus new therapies that also target influenza B, and so could be used empirically, are particularly valuable. A limitation of this study is that we have not assessed activity against a panel of influenza B viruses, but we have determined that H84T is efficacious against representatives of the two influenza B lineages, B/Brisbane/60/2008 (Victoria lineage) and B/Florida/4/2006 (Yamagata lineage).

Paralleling the reduced mitogenicity of H84T compared to wild-type BanLec that we previously demonstrated in vitro, systemic administration of H84T does not result in the robust inflammatory response seen after administration of the wild-type lectin, indicating that we have truly removed mitogenicity from H84T by substituting one specific amino acid for another. Mitogenicity has primarily been addressed as an in vitro concept, with studies examining mitogenicity of lectins in vivo focusing on local rather than systemic effects (87). However, through our study, we have been able to characterize in vivo the effects of a systemically delivered mitogenic versus non-mitogenic lectin. Lessening mitogenic activity of BanLec via the H84T mutation has removed a major hurdle in the development of an antiviral lectin for clinical use, since mitogenicity has been viewed as the biggest drawback (48). In addition, we have shown that H84T BanLec is very safe when delivered by the IP and SC routes, with our previous study as well as this study showing that it is also safe when administered intranasally.

As demonstrated by the single dose pharmacokinetics, H84T delivered systemically by the IP route possesses a long terminal half-life, indicating that infrequent or even single dosing could potentially be efficacious, which would be clinically advantageous. However, IV administration, which is largely analogous to IP administration in the mouse, could not generally

be used to treat outpatients with influenza virus infections and is not likely the best strategy for all clinical situations. Oral administration is not a feasible clinical strategy, as it is known that alimentary lectins do not effectively distribute to the blood (51–53), but as we have shown, SC administration is efficacious and has potential as an eventual treatment in the outpatient setting. Thus, H84T BanLec shows promise for use in both hospitalized patients and outpatients. It is notable and promising that administration of H84T can be delayed for up to 72 hours and still offer 80% protection by the IP route and 50% protection by the SC route. It is important to note that people have antibodies against banana lectin (75), which means that they would potentially develop or already possess antibodies against H84T, but this is not expected to limit activity given that the efficacy of H84T against influenza infection was not lessened in mice with anti-H84T antibodies. Of course, this would ultimately need to be determined in humans.

Our work indicates that H84T binds HA specifically, as binding to HA can be inhibited by a known ligand of BanLec but not by a non-interacting monosaccharide, and that it functions as an anti-influenza agent via fusion inhibition. Furthermore, carbohydrate binding is essential for both binding and fusion inhibition, as the carbohydrate binding site mutant D133G does not bind as efficiently and is not inhibitory to fusion. A key remaining question is where H84T might bind HA, as both its head and stalk regions are glycosylated with high-mannose type *N*-glycans (2), among other glycans, which are ligands for H84T. Neutralizing antibodies that function as fusion inhibitors typically bind the stalk of HA (88–90), which contains the fusion peptide and other components necessary for fusion (91). The stalk contains a greater number of conserved glycosites than the head and glycans in the stalk are key for proper folding of HA and its transport to the surface of the virus particle (24, 25, 92), which means that it would be potentially more difficult for viruses to escape an agent that binds to the stalk than an agent that binds to the

head. Indeed, recent work suggests that broadly neutralizing antibodies that bind to the stalk of HA are quantifiably harder to escape than antibodies that bind to the head of HA (93). Since H84T inhibits fusion and inhibits a wide range of viruses, we hypothesize that it binds at least the more highly conserved stalk of HA, perhaps not to the exclusion of binding to the head, and that it would be difficult for viruses to escape its inhibition. A potential limitation of H84T is that it may require that its target be glycosylated, and pandemic strains are sometimes less heavily glycosylated than seasonal strains, but some glycosylation of the stalk is virtually always present, even in pandemic strains (2). Interestingly, the number of glycosites that a certain strain possesses seems to correlate with the IC_{50} concentration of H84T against that strain. Contemporary H3 viruses have more glycosites than contemporary H1 viruses (2) and H84T has a lower IC_{50} concentration against the former strains, which correlates with the higher amount of methyl α-D-mannopyranoside needed to compete for binding to H3 versus H1 HA.

H84T treatment, regardless of infection status, enlarges the LAMP1-positive compartment, consistent with the observation that many lectins are internalized by endocytosis and that some induce the formation of large lysosomes (85, 86). H84T and to a much lesser extent D133G localize to the late endosome/lysosome. Although H84T is internalized into the endosomal compartment and enlarges it, the fact that fusion at the plasma membrane is inhibited by H84T (Figure 2.6), in addition to uncoating at the endosomal membrane, suggests that the anti-influenza activity of H84T does not depend primarily on alteration of the endosomal compartment. Consistent with these observations, pre-conditioning of the endosomal compartment with H84T is not required for viral inhibition, since either cells or virus can be pre-treated with H84T and the lectin is still highly active against uncoating. We therefore posit that binding of H84T to HA is important for the inhibitory effect of H84T. We propose a model in

which H84T, internalized in both the presence and absence of virus, likely by endocytosis, accumulates in the late endosomal/lysosomal compartment where fusion occurs and is thus positioned at a key watch point to interact with HA and thereby prevent entry of virus into the cytoplasm. Since H84T disrupts fusion of the virus and prevents its release into the cytoplasm, it is reasonable to think that the virus might be degraded once it reaches the lysosome, accounting for the ability of H84T to decrease influenza virus replication overall.

Our data demonstrate that H84T BanLec has great potential as a new antiviral against influenza viruses. It is very well tolerated and non-mitogenic in vivo and is highly efficacious against otherwise lethal influenza virus infection via three distinct routes of administration, even when treatment is delayed: IN, IP, and SC, the latter two of which are especially clinically relevant. H84T is highly broad-spectrum in that it inhibits replication of all oseltamivir-resistant and -sensitive strains and all influenza A and B strains tested, highlighting its promise as an empiric drug for influenza illness, which will be critically needed in the event of a new pandemic influenza virus or increasing resistance to neuraminidase inhibitors. Remarkably, H84T is broad-spectrum not only in its anti-influenza activity, but also in the sense that it inhibits HIV and HCV as reported previously (60), as well as MERS and SARS (J. Chan and D. Markovitz, manuscript in preparation), and Ebola (E. Covés-Datson, J. White, and D. Markovitz, manuscript in preparation), among other viruses. The present study, along with our previous work, underscores the value of engineering antiviral lectins to be non-mitogenic and safe in vivo, as H84T and perhaps eventually other similarly engineered lectins could be leveraged as a therapeutic arsenal against a diverse array of viruses.

2.6 Materials and Methods

2.6.1 H84T and D133G BanLec purification

Recombinant His-tagged H84T and D133G were prepared from *E. coli* as previously described (60), except that non-His-tagged H84T, which was used in experiments unless otherwise stated, was prepared using a Sephadex G-75 column instead of a Ni-NTA agarose column. Briefly, to produce non-His-tagged proteins, cleared lysates were added to a Sephadex G-75 column that had been equilibrated with PBS. The column was then washed with PBS until the OD of the flow-through at 280 nm was less than 0.02. Elution of the protein was then performed using 0.2 M methyl α-D-glucopyranoside. For all lectins, endotoxin testing was performed using the Pierce LAL Chromogenic Endotoxin Quantitation Kit (Thermo Fisher Scientific). Endotoxin removal was performed by adding glucose to a 1 M concentration and passing pooled eluates containing protein through Mustang E filters (Pall). Following endotoxin removal to < 0.1 endotoxin units/mg of protein, the Vivaspin 20 centrifugal unit with 3K MWCO was used to remove glucose and concentrate the lectin in water. Protein and endotoxin concentrations were then measured by BCA and LAL assays, respectively.

2.6.2 Cells and viruses

Madin-Darby canine kidney (MDCK) cells were maintained in Dulbecco's Modified Eagle Medium (DMEM, Gibco) supplemented with 10% FBS and 1% penicillin/streptomycin at 37ºC in 5% CO_2. Influenza virus infection was performed on monolayers of MDCK cells in virus growth buffer (DMEM supplemented with 0.187% BSA and 25 mM HEPES). Supernatant from 293T cells transfected with eight influenza gene plasmids was used to propagate A/WSN/33

(H1N1) on MDCK cells as previously described (94). Recombinant virus containing HA and NA genes from A/Colorado/15/2014 (H3N2) and other genes from A/Puerto Rico/8/1934 (H1N1) was engineered by reverse genetics and propagated on MDCK-SIAT1 cells to limit adaptation and glycan changes. Influenza A Virus, A/Perth/16/2009 (H3N2), FR-370, Influenza A Virus, A/Florida/3/2006 (H1N1), FR-364, Influenza A Virus, A/Louisiana/08/2013 (H1N1)pdm09, FR-1440, Influenza A Virus, A/Texas/12/2007 (H3N2), FR-1442, and Influenza B Virus, B/Brisbane/60/2008 (Victoria Lineage), FR-177, were obtained through the Influenza Reagent Resource, Influenza Division, WHO Collaborating Center for Surveillance, Epidemiology and Control of Influenza, Centers for Disease Control and Prevention, Atlanta, GA, USA and propagated one to two times on MDCK cells. Virus titers were determined by $TCID_{50}$ assay and converted to estimated plaque-forming units (PFU) by the conversion $TCID_{50} \approx 0.7$ PFU.

2.6.3 ELISA for determination of H84T binding to HA

96-well ELISA plates (Thermo Fisher Scientific) were coated overnight with 100 ng recombinant H1 or H3 HA proteins from Influenza A/California/07/2009 (H1N1)pdm09 and Influenza A/Perth/16/2009 (H3N2), respectively, produced in baculovirus. All steps were performed at room temperature. Recombinant H1 HA with Histidine Tag, from Influenza A/California/07/2009 (H1N1)pdm09, FR-559, and recombinant H3 HA with Histidine Tag, from Influenza A/Perth/16/2009 (H3N2), FR-472, were obtained through the Influenza Reagent Resource, Influenza Division, WHO Collaborating Center for Surveillance, Epidemiology and Control of Influenza, Centers for Disease Control and Prevention, Atlanta, GA, USA. Following overnight incubation with HA, ELISA plates were washed with PBS 5 times before being blocked for 2 h in PBS containing 2% bovine serum albumin. After 5 washes in PBS, H84T or

D133G BanLec (0.0001-10 μM) was added to the wells in dilution buffer (PBS containing 0.05% Tween-20 and 2% fetal bovine serum) and incubated for 2 h. Plates were then washed before the addition of rabbit polyclonal anti-BanLec antibody diluted 1:4000 in dilution buffer. Following a 45 min incubation, plates were washed and biotinylated goat anti-rabbit antibody (Jackson ImmunoResearch Laboratories) added to wells at 1:200,000 in dilution buffer for 45 min. Plates were washed again before HRP-conjugated streptavidin was added at 1:300 in dilution buffer for 45 min. After a final set of washes, prepared TMB (BioRad) was added to wells for colorimetric analysis and absorbance measured at 450 nm. To assess whether carbohydrates could inhibit the interaction between H84T BanLec and influenza HA, a fixed concentration of lectin was used (0.1 μM) and was pre-incubated with methyl α-D-mannopyranoside (0.0001-0.1 μM), galactose (0.0001-0.1 μM), or yeast mannan (approximately 0.00001-0.01 μM) before being added to the HA-coated wells.

2.6.4 Virus infection and immunofluorescence staining

MDCK cells were plated in 8-well chamber slides, pre-treated for 1 h with 0.05-10 μM H84T, 10 μM D133G, or 40 μM arbidol (ARB), and infected at 37ºC with A/WSN/1933 (H1N1), A/Perth/2009 (H3N2), or A/Florida/2006 (H1N1) at a multiplicity of infection (MOI) of 0.5 in the presence of H84T, D133G, or ARB for 2.5 h to examine uncoating or 5 h to examine viral protein expression. Where indicated, virus alone (rather than cells) was pre-treated with H84T, D133G, or ARB and uncoating examined. For M1/LAMP1 colocalization studies, following pre-treatment cells were incubated with A/WSN/1933 (H1N1) at 4ºC for 1 h to allow only for attachment and to synchronize infection, excess virus was removed, treatment-containing medium was replaced, and the cells were incubated at 37ºC for an additional 3 h. Spreading

infections of B/Brisbane/60/2008 were performed following pre-treatment, removal of excess virus following 1 h of incubation, and replacement of treatment-containing medium at MOI = 0.05 for 16-18 h. Infected cells were washed twice in virus growth buffer and once in PBS before fixation in 2% PFA/PBS. For immunofluorescence assays, after fixation cells were blocked in 3% BSA/PBS, permeabilized in 0.1% Triton X-100, and incubated with mouse anti-M1 matrix antibody (Takara), rabbit anti-LAMP1 antibody (Abcam), pooled mouse anti-influenza A protein antibodies, or pooled mouse anti-influenza B protein antibodies for 1 hour. Mouse Monoclonal Antibody Influenza Type A (Pool), FR-51 and Mouse Monoclonal Antibody Influenza Type B (Pool), FR-829, were obtained through the Influenza Reagent Resource, Influenza Division, WHO Collaborating Center for Surveillance, Epidemiology and Control of Influenza, Centers for Disease Control and Prevention, Atlanta, GA, USA. Following 1 wash in 3% BSA/PBS and 2 washes in PBS, cells were incubated with the appropriate secondary antibody, goat anti-mouse AlexaFluor 488 or goat anti-rabbit AlexaFluor 594, for 30 minutes. Slides were mounted using Prolong Gold Antifade Reagent with DAPI (Thermo Fisher Scientific). Immunofluorescence was visualized by confocal microscopy on a Nikon A-1 instrument.

2.6.5 In vitro cytotoxicity in MDCK cells

Monolayers of MDCK cells in 96-well plates were treated for 24 h with H84T or D133G BanLec (0-15 μM) in 100 μl medium. Cytotoxicity was evaluated by MTT assay (Roche) per manufacturer's instructions. Briefly, cells were incubated for 4 h at 37ºC with 10 μl MTT labeling reagent and resulting formazan salt crystals solubilized with 100 μl 10% SDS in 0.01 M HCl. After overnight incubation at 37ºC to fully solubilize the crystals, absorbance was measured at 595 nm.

2.6.6 Cell-associated virus assay

Virus was incubated with 0, 1, 10, 100, 1000, or 10,000 nM H84T with or without 10 μg/ml H17-L19 monoclonal antibody for 30 minutes at room temperature, after which the virus-H84T mixture was incubated with MDCK cells for 1h at 4ºC, allowing only for attachment. Following 3 washes with cold virus growth buffer, cells were collected in Trizol reagent (Thermo Fisher Scientific) and whole cell RNA extracted. To measure the relative amount of cell-associated virus normalized to *GAPDH* expression, qRT-PCR was performed using primers specific to influenza A *M1* and to *GAPDH*. Primers to influenza A *M1* (forward primer: 5′ AAG ACC AAT CCT GTC ACC TCT GA 3′, reverse primer: 5′ CAA AGC GTC TAC GCT GCA GTC C 3′) and to *GAPDH* (forward primer: 5′ ACA TCG CTC AGA CAC CAT G 3′, reverse primer: 5′ TGT AGT TGA GGT CAA TGA AGG G 3′) were used.

2.6.7 Hemagglutination inhibition assay

Three-fold serial dilutions of H84T were pre-incubated with virus, with turkey red blood cells (RBCs), or with both RBCs and virus before the H84T-virus mixture was added to RBCs, H84T-RBC mixture was added to virus, or the H84T-virus and H84T-RBC mixtures were added together in 96-well V-bottom plates. Three dilutions of A/WSN/1933 (H1N1) virus were used (1:8, 1:16, and 1:32). Plates were gently tapped to mix and then incubated for 30 min at room temperature. Hemagglutination was assessed visually.

2.6.8 Virus-cell fusion assay

MDCK cells were pretreated for 1 hour with 1 or 10 μM H84T or 20 or 40 μM of the fusion inhibitor arbidol (ARB, Cayman Chemical), incubated with octadecyl rhodamine (R18, Sigma-

Aldrich)-labeled A/WSN/1933 virus for 1 hour at 4ºC to allow attachment of the virus, then washed three times in virus growth buffer and once in PBS to remove unbound virus. Fluorescence dequenching was assessed as previously described (83). Briefly, viral fusion to the cell membrane was triggered at 37ºC using fusion buffer (150 mM NaCl solution with 25 mM HEPES, Corning) at pH ~5.25. Fluorescence dequenching of R18 was monitored on a microplate fluorometer with excitation and emission wavelengths of 560 and 590 nm, respectively. Maximal dequenching was achieved with 1% Triton X-100 set at 100%.

2.6.9 Safety of intraperitoneal H84T

8-week-old female BALB/c mice were injected intraperitoneally (IP) with two 50 mg/kg doses of WT, H84T, or D133G BanLec administered one month apart (n = 10 per group) and weighed and scored for appearance and injection site lesions.

2.6.10 Pharmacokinetics of single dose intraperitoneal (IP) H84T

To determine the dose-dependent pharmacokinetic profile of H84T following a single IP dose, groups of 44 5-week-old male CFW mice were injected IP on a single occasion with 5, 15, or 50 mg/kg H84T in PBS. Plasma and lung samples from multiple time points were processed and analyzed by ELISA. *Plasma and lung sample processing:* Blood samples (0.5-1 ml) were collected via cardiac puncture tubes and deposited into K3 EDTA tubes and mice euthanized at 0, 5, 15, and 30 minutes and 1, 2, 4, 8, 24, 48, and 72 hours post-dose (n = 4 per time point) for collection of liver and lungs. Blood samples were placed on ice and centrifuged at 2500 rpm for 10 minutes under refrigerated conditions, after which plasma was collected and frozen at -80ºC within 1 hour of collection. Liver and lungs were rinsed with 0.9% sodium chloride, blotted dry,

and weighed. Mouse lung tissue was weighed (5 mg) and homogenized in 1mL of PBS with 1M glucose and complete EDTA free protease inhibitor cocktail. The homogenized tissue was incubated on ice for 1 h to allow greater extraction of H84T and centrifuged at 10,000 rpm for 10 min at 4ºC. The supernatant was transferred to clean 1.5 mL vials and cleared by centrifuging again at 15,000 rpm for 10 minutes at 4ºC. *ELISA:* Standard curves were prepared in duplicate in mouse plasma or lung homogenate and quality control samples analyzed in addition to unknown samples. 96-well Nunc MaxiSorp plates (Thermo Fisher Scientific) were coated with 100 ng of capture antigen, HIV gp120, and sealed and incubated overnight at 4ºC. The capture antigen was aspirated and discarded, and the wells were washed 3 times with wash buffer (0.05% Tween-20 in PBS). The wells were blotted dry, filled with blocking buffer (3% BSA in PBS), and incubated at room temperature (RT) for 2 h. After 3 more washes, 100 µl mouse plasma or processed mouse lung tissue supernatant were added to each well and the plate was incubated at RT for 1 h on a mini blot rocker. The wells were washed with wash buffer 6 times and the primary antibody (rabbit polyclonal anti-BanLec at 1:25,000) in blocking buffer was added and incubated at RT for 1 h on a mini blot rocker. The wells were then washed with wash buffer 8 times and secondary antibody (biotinylated goat anti-rabbit at 2 µg/ml) in blocking buffer was added and incubated for 30 min at RT on a mini blot rocker. The wells were washed with wash buffer 8 times and detection antibody (high sensitivity HRP-conjugated streptavidin, 1:200 for plasma and 1:400 for lung) was added and incubated at room temperature for another 30 min on a mini blot rocker. After a final set of 8 washes, the substrate-chromogen TMB was added and incubated at room temperature for 10-20 min in the dark. The reaction was stopped by the addition of stopping solution (0.5M H_2SO_4) and read at 450 nm on a plate reader. The following PK parameters were calculated using the Phoenix WinNonLin Non-compartmental Analysis

program, version 6.4.0.768: maximum concentration, C_{max} (ng/ml or ng/g); time at which maximum concentration occurs, T_{max} (hrs); area under the curve, AUC (ng*hrs/ml); half-life, $t_{1/2}$ (hrs).

2.6.11 Distribution of single dose intraperitoneal (IP) H84T

To determine the distribution of H84T following a single IP dose, 15-week-old female 129svev/B6 mice were injected IP with 50 mg/kg H84T. Mice were culled at 4 time points post injection (6h, 12h, 24h, and 48h) and lungs, liver, kidneys, heart, spleen, and brain harvested and snap frozen. Frozen organs were homogenized on dry ice by mortar and pestle and protein extraction performed in the presence of protease inhibitors. Protein extracts were separated by 4-20% SDS-PAGE and immunoblotted using rabbit anti-BanLec polyclonal antibody and HRP-conjugated anti-rabbit secondary antibody.

2.6.12 Therapeutic efficacy of systemic H84T against influenza in BALB/c mice

Animals: Female 18-20 g BALB/c mice were obtained from Charles River Laboratories (Wilmington, MA). *Virus:* Influenza A/WSN/HA(NC/2099-N225G)/1933 virus. Recombinant influenza A/WSN/33 (H1N1) virus containing the HA gene of influenza A/New Caledonia/20/99 (H1N1) was generated by reverse genetics as described previously (94, 95). The Asp225Gly mutation was introduced in the HA gene encoding the HA1 subunit by PCR based site-directed mutagenesis by Dr. Larissa Gubareva (CDC, Atlanta, GA). The recombinant virus was designated influenza A/WSN/33 HAnc-Asp225Gly (H1N1) and became lethal after 7 serial passages in the lungs of animals. Virus was plaque purified and a virus stock was prepared by growth on MDCK cells. *Experimental design:* For the intraperitoneal (IP) efficacy study, groups

of 10 mice were treated by the IP route on a single occasion with a 5, 15, or 50 mg/kg dose of H84T at 24 hours pre-virus challenge, or once daily with 0.15, 0.5, 1.5, or 5.0 mg/kg doses of H84T, beginning 4 hours post-virus challenge, or once per day by the IP route for 5 days beginning 4, 24, 48, or 72 hours post-challenge. Additional groups of mice were also treated IP on a single occasion with 50 mg/kg H84T 21 days pre-virus challenge, then once daily for 5 days with 5.0 mg/kg H84T. Control groups included mice treated with 10 mg/kg/day oseltamivir twice per day for 5 days beginning 4, 24, 48, or 72 hours post-infection, or placebo (15 mice) treated BID for first 5 days post-infection, then QD for next 3 days to match treatment beginning at 4 hours post-infection and 72 hours post-infection. For the subcutaneous (SC) efficacy study, mice were treated by SC injection using a 50 mg/kg dose of H84T either once or twice within four days post-infection. A group of ten mice was given oseltamivir by oral gavage (PO) twice daily for 5 days with 10 mg/kg of oseltamivir, starting 48 hours post-infection. Control mice treated with physiological sterile saline as placebo were dosed according to the same regimen as H84T. In each study, five non-treated normal control mice were maintained for weight comparison. For influenza virus challenge, mice were anesthetized by IP injection of ketamine/xylazine (50 mg/kg//5 mg/kg) prior to challenge by the intranasal route with approximately 5 x 10^3 (2 x LD_{50}) cell culture infectious doses ($CCID_{50}$) (IP efficacy) or 1 x 10^3 $CCID_{50}$ (SC efficacy) of virus per mouse in a 90 µl inoculum volume. Mice were weighed prior to treatment and then every other day thereafter to assess the effects of treatment on ameliorating weight loss due to virus infection. All mouse groups were observed for morbidity and mortality through day 21 post-infection.

2.6.13 Therapeutic efficacy of intranasal H84T against H3N2 influenza virus

Mouse-adapted influenza A/Hong Kong/8/1968 (H3N2) virus was kindly provided by Dr. Brian E. Gilbert, Baylor College of Medicine. As previously described (96), frozen stock (2.8 $x10^7$ 50% tissue culture infective doses [$TCID_{50}$]/ml) of virus was diluted 1:250 in 0.05% gelatin in Eagle's minimal essential medium and delivered by aerosolization for 20 min to achieve the 90% lethal dose (LD_{90}) to LD_{100} (~100 $TCID_{50}$ per mouse) in wild type six week-old C57BL/6J mice of a single sex. For each group, $n = 12$. Animals were examined and weighed daily and sacrificed if they met euthanasia criteria, including signs of distress or loss of 30% preinfection body weight. Mice were treated daily for 5 days beginning 4 hours post-infection with 40 μL intranasal PBS (sham) or H84T BanLec (0.1 mg/kg) without anesthesia.

2.6.14 Animal care and use

The IP and SC efficacy studies were conducted in accordance with the approval of the Institutional Animal Care and Use Committee of Utah State University dated September 2, 2016 (expires Sept. 1, 2019). The work was done in the AAALAC-accredited Laboratory Animal Research Center of Utah State University. The U.S. Government (National Institutes of Health) approval was renewed April 7, 2013 (Animal Welfare Assurance no. A3801-01) in accordance with the National Institutes of Health Guide for the Care and Use of Laboratory Animals (Revision; 2011). The in vivo safety and distribution studies were conducted in accordance with the approval of the Institutional Animal Care & Use Committee of the University of Michigan.

2.6.15 Statistics

All statistical analyses were performed using GraphPad Prism 6 and 7. Specific tests used are noted in figure legends. All *t* tests performed were two-tailed.

2.6.16 Data availability

H84T must be obtained through an MTA.

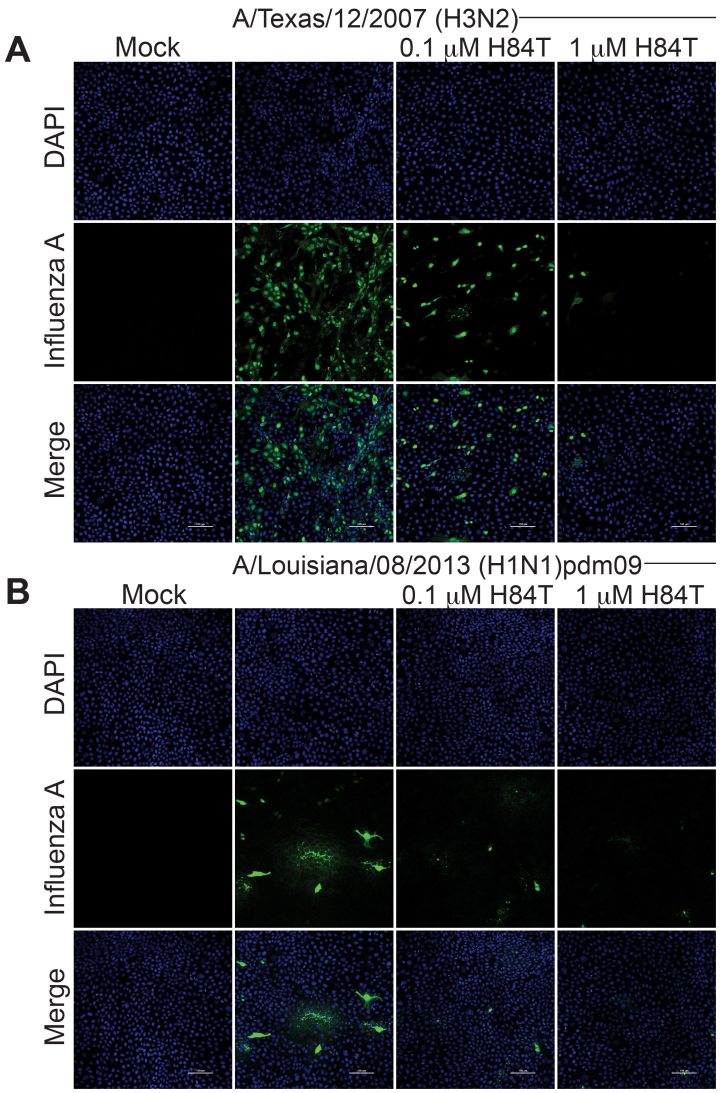

Figure 2.1 H84T decreases spreading infection of oseltamivir-resistant influenza strains.

Representative immunofluorescent micrographs of influenza A antigen staining (green) and nuclei (blue) 16-18 h post-infection. MDCK cells were pre-treated for 1 h with 0.1 or 1 μM H84T and infected with the oseltamivir-resistant strains A/Texas/12/2007 (H3N2) (A) or A/Louisiana/08/2013 (H1N1)pdm09 (B) at MOI = 0.05 for 16-18 h. Data are representative of two independent experiments.

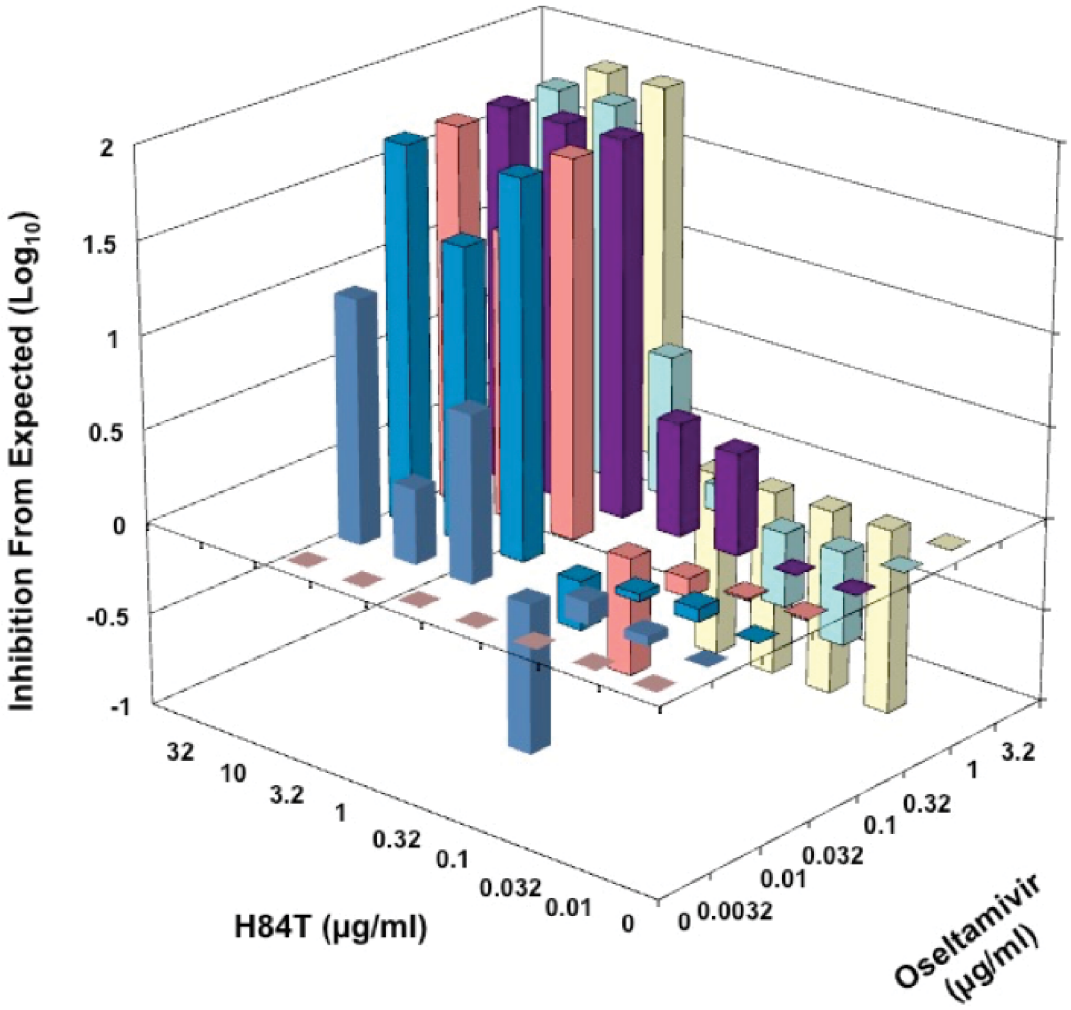

Figure 2.2 H84T and oseltamivir exhibit minor synergy against A/California/07/2009 (H1N1)pdm09 virus.

Three-dimensional MacSynergy™ II plot showing dual drug interactions of H84T and oseltamivir carboxylate. MDCK cells were infected with influenza A/California/07/2009 (H1N1)pdm09 virus and treated with dual drug combinations. The X- and Y-axis are the concentrations of H84T and oseltamivir, respectively. The Z-axis is the calculated drug-drug interaction based on Bliss independence and expressed as inhibition from expected. The null reference plane represents no interactions whereas bars above, or below the null reference plane represent significant interactions. Synergy volume was 36.32 $\mu M^2\%$, indicative of minor but significant synergy. Experiment performed by D.F.S.

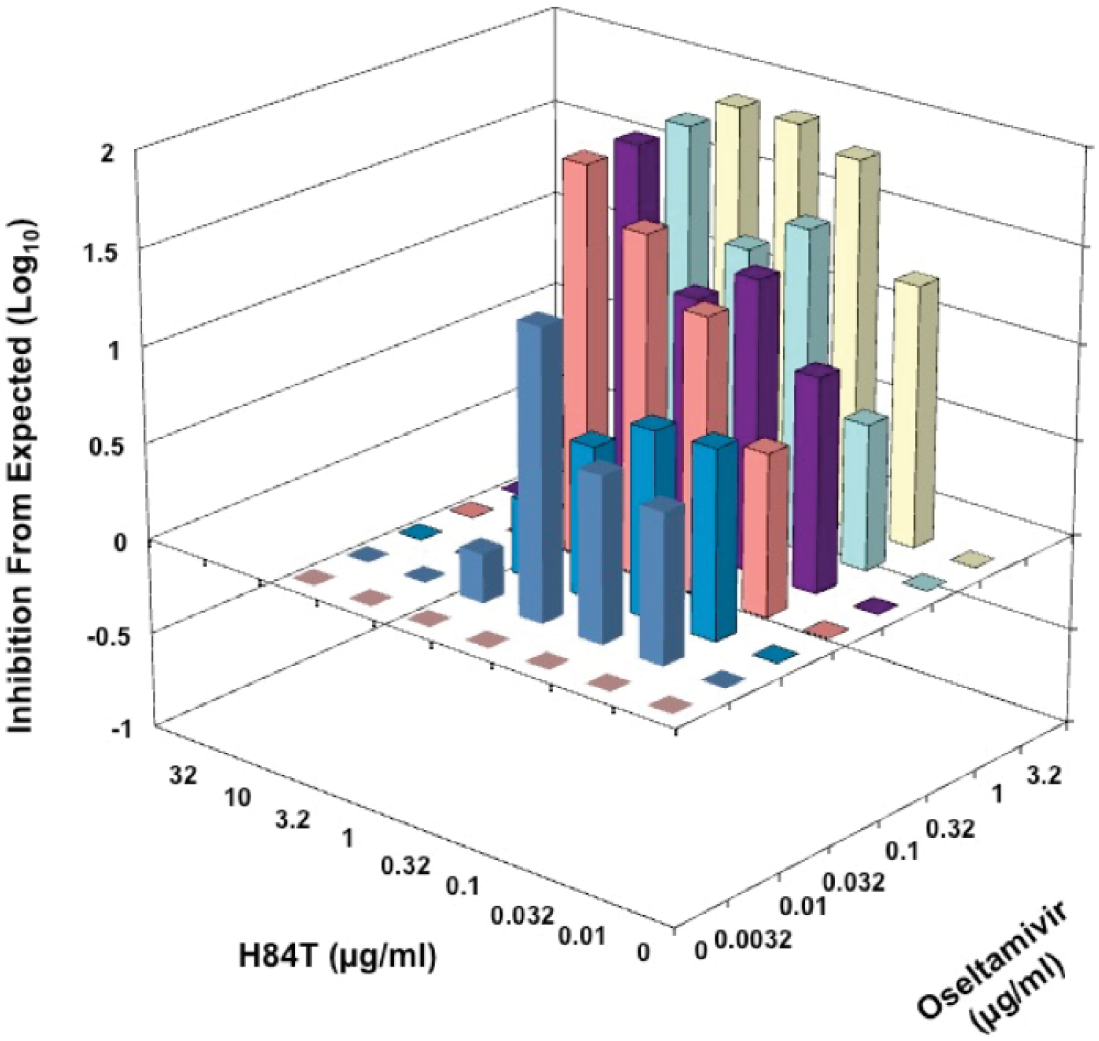

Figure 2.3 H84T and oseltamivir exhibit minor synergy against A/Perth/16/2009 (H3N2) virus.

Three-dimensional MacSynergy^{TM} II plot showing dual drug interactions of H84T and oseltamivir carboxylate. MDCK cells were infected with influenza A/Perth/16/2009 (H3N2) virus and treated with dual drug combinations. The X- and Y-axis are the concentrations of H84T and oseltamivir, respectively. The Z-axis is the calculated drug-drug interaction based on Bliss independence and expressed as inhibition from expected. The null reference plane represents no interactions whereas bars above, or below the null reference plane represent significant interactions. Synergy volume was 29.54 $\mu M^2\%$, indicative of minor but significant synergy. Experiment performed by D.F.S.

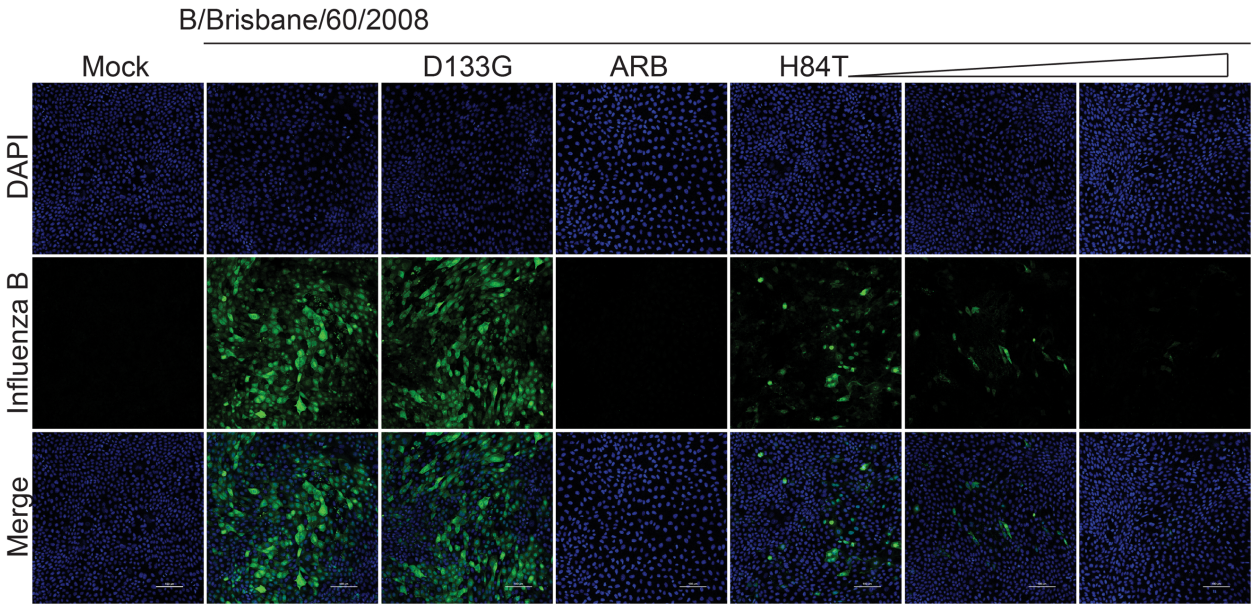

Figure 2.4 H84T decreases spreading infection of influenza B virus.

Representative immunofluorescent micrographs of influenza B antigen staining (green) and nuclei (blue) 16-18 h post-infection. MDCK cells were pre-treated for 1 h with 0.1, 1, or 10 μM H84T, or 40 μM of the fusion inhibitor arbidol (ARB) and infected with B/Brisbane/60/2008 at MOI = 0.05 for 16-18 h. Data are representative of two independent experiments.

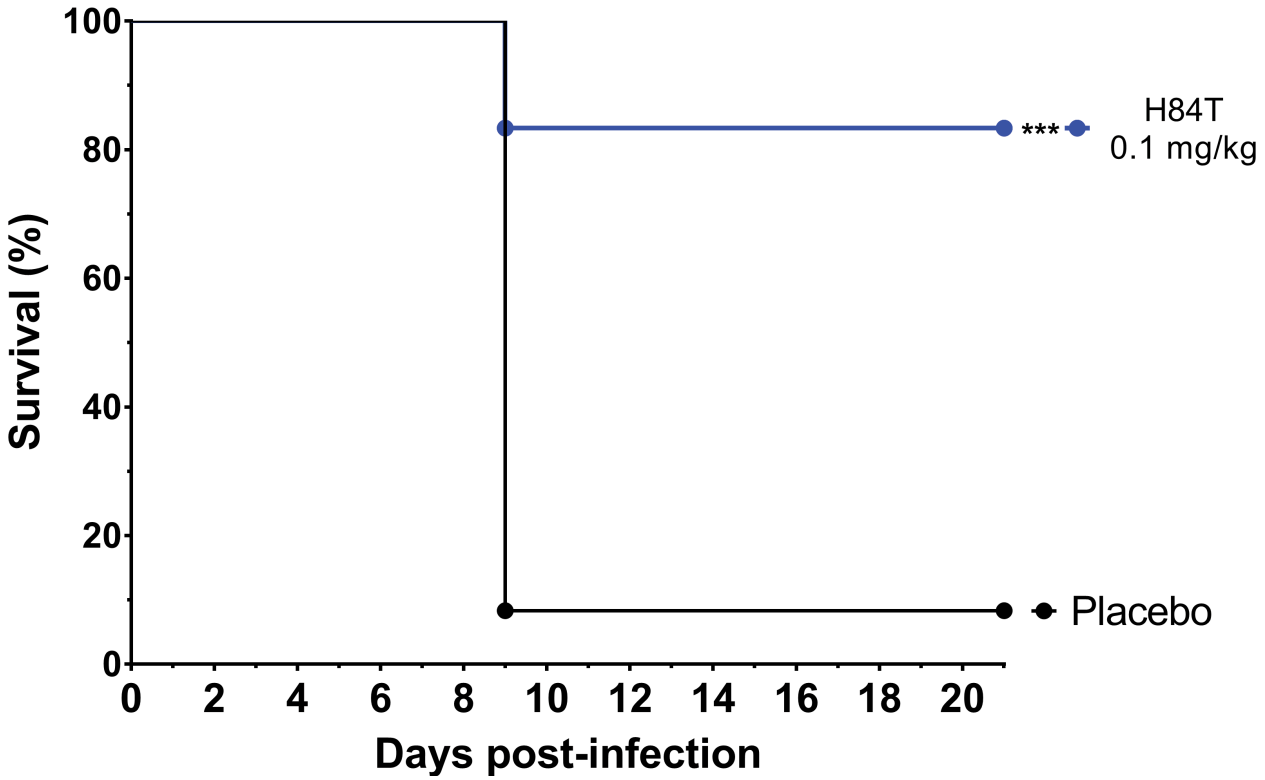

Figure 2.5 Intranasal H84T is efficacious against lethal H3N2 influenza virus infection.

Survival of C57BL/6J mice challenged by aerosolization with 90% to 100% mouse lethal dose of mouse-adapted A/Hong Kong/8/1968 (H3N2) following intranasal treatment with H84T (0.1 mg/kg) or PBS (placebo) once daily for 5 days beginning 4 h post-challenge. ***$P < 0.001$. The Kaplan-Meier survival curve was compared by the log-rank (Mantel-Cox) test followed by pairwise comparison using the Gehan-Breslow-Wilcoxon test. Experiment designed by V.V.K. and S.E.E. and performed by V.V.K. and J.P.G.

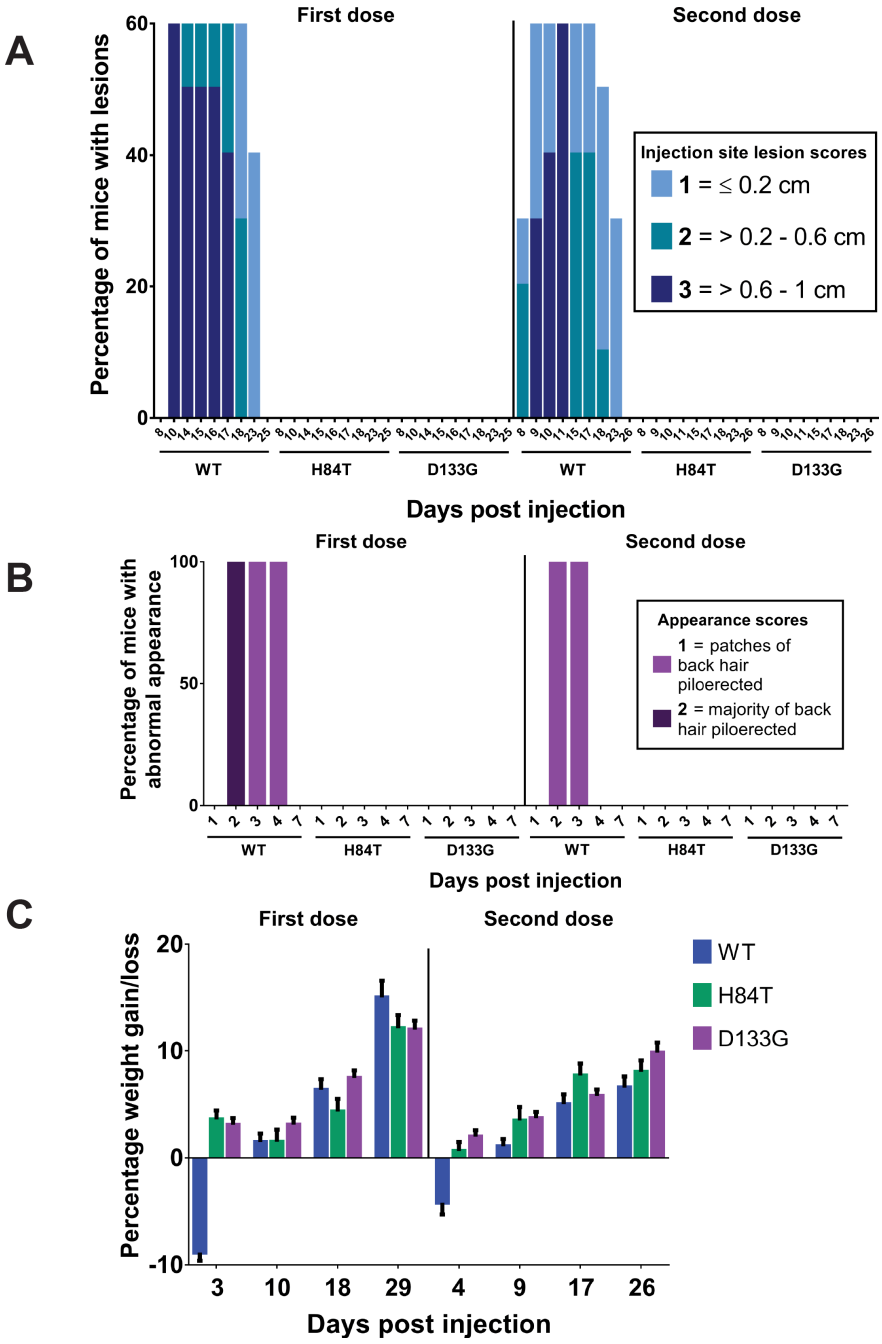

Figure 2.6 Systemic H84T is very well tolerated in mice.

(**A** to **C**) BALB/c mice were injected intraperitoneally (IP) with two 50 mg/kg doses of WT, H84T, or D133G BanLec administered one month apart (n = 10 per group). Injection site lesions (**A**) and appearances (**B**) were scored, and weight measured (**C**) for all mice for 59 days post-injection. In (C), the data represent the mean for all mice in each group and error bars the standard error of the mean. Experiment performed by M.L.

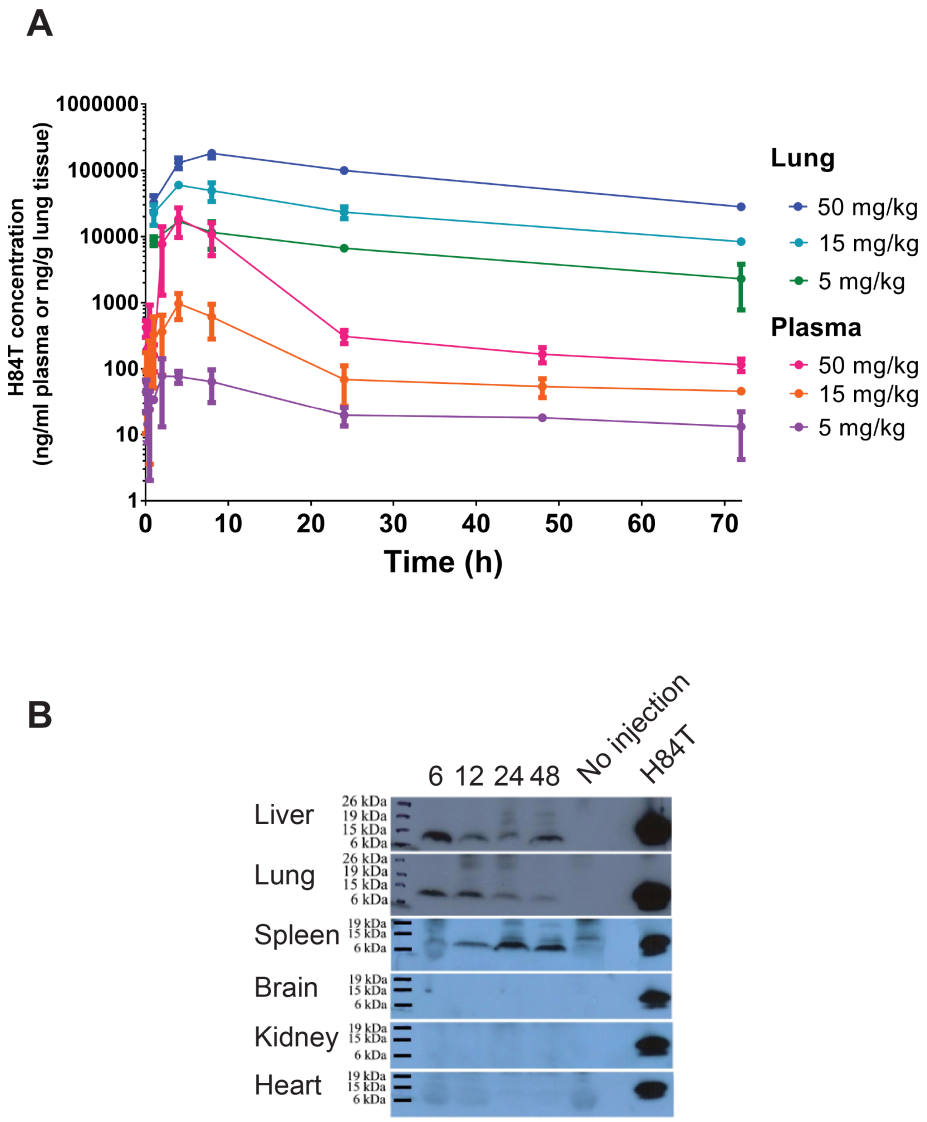

Figure 2.7 H84T distributes to the lung and has a long serum and tissue half-life.

(**A**) Concentration of H84T in the lung and plasma of male CFW mice following intraperitoneal administration of 5, 15, or 50 mg/kg H84T. Plasma and lungs were collected at 11 time points and the concentration of H84T determined by ELISA. Data points represent mean ± standard deviation ($n = 4$ per group). (**B**) Immunoblots of H84T distribution to liver, lung, spleen, brain, kidney, and heart. 15-week-old female 129svev/B6 mice were injected with 50 mg/kg H84T IP. Mice were culled at 4 time points post-injection (6 h, 12 h, 24 h, and 48 h) and organs harvested for protein extraction and immunoblotting. Experiments performed by S.M.C. and E.L. (A), and M.L. (B).

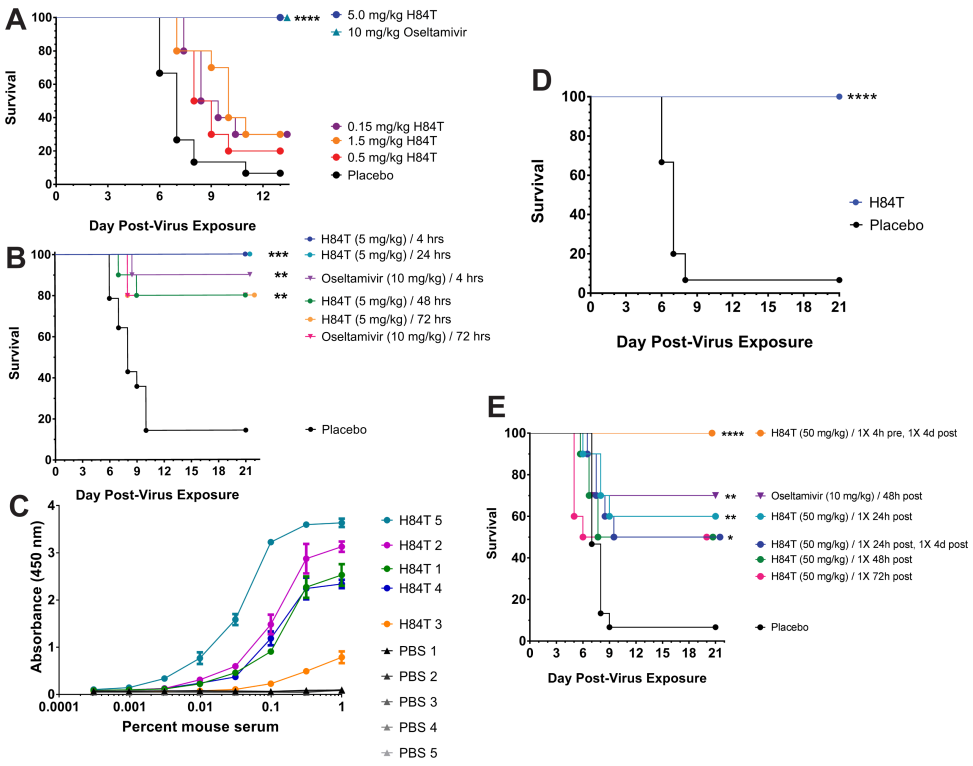

Figure 2.8 Systemic H84T treatment is highly efficacious against lethal influenza virus infection in mice.

(**A, B, D**) Therapeutic efficacy of H84T administered intraperitoneally in BALB/c mice challenged intranasally with 2 times the 50% mouse lethal dose of A/WSN/HA(NC/2099-N225G)/1933 (H1N1). (**A**) Survival of mice following IP treatment with H84T (mg/kg) once daily for 5 days beginning 4 h post-challenge. (**B**) Survival of mice following IP treatment with H84T (5 mg/kg) once daily for 5 days beginning 4, 24, 48, or 72 h post-challenge, or with oseltamivir (10 mg/kg) beginning 4 or 72 h post-challenge. (**C**) BALB/c mice were injected with PBS or 50 mg/kg H84T (n = 5 per group) and sera collected 21 days post-injection for detection of anti-H84T antibodies by ELISA. A fixed amount (100 ng) of H84T was used to coat plates and diluted sera used as the primary antibody. Data are representative of one independent experiment performed in triplicate. (**D**) Survival of mice following IP treatment with H84T (50 mg/kg) on a single occasion 21 days before challenge, then once daily for 5 days (5 mg/kg/day) beginning 4 h post-challenge. Placebo mice received PBS 21 days pre-challenge and once daily for 5 days beginning 4 h post-challenge. (**E**) Therapeutic efficacy of H84T administered subcutaneously (SC) in BALB/c mice challenged intranasally with a lethal dose of A/WSN/HA(NC/2099-N225G)/1933 (H1N1). Survival of mice following SC treatment with a regimen of either one or two 50 mg/kg doses of H84T within four days post-infection. $*P < 0.05$, $**P < 0.01$, $***P < 0.001$, and $****P < 0.0001$. Kaplan-Meier survival curves for A to D were compared by the log-rank (Mantel-Cox) test followed by pairwise comparison using the Gehan-Breslow-Wilcoxon test. Experiments performed by E.B.T. (A, B, D, and E) and S.R.K. (C).

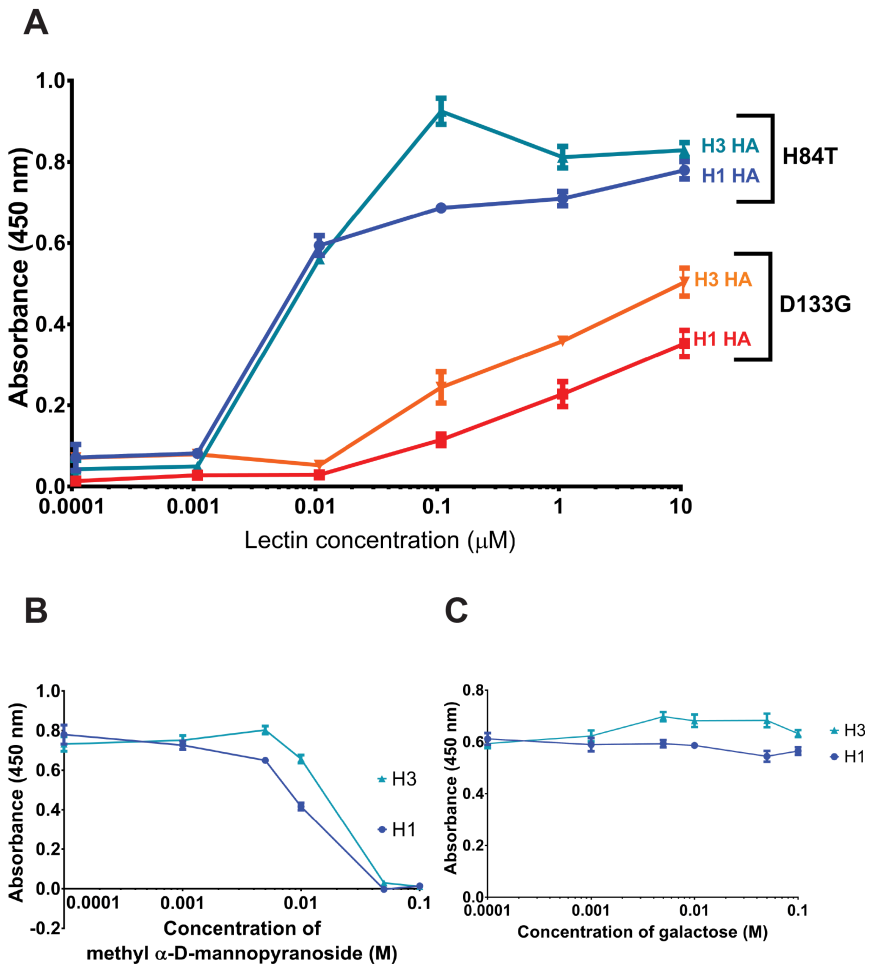

Figure 2.9 H84T specifically binds to influenza HA.

(**A**) H84T and D133G binding to HA as measured by ELISA. A fixed amount (100 ng) of recombinant glycosylated H1 or H3 HA proteins from A/California/07/2009 (H1N1)pdm09 and A/Perth/16/2009 (H3N2), respectively, was used to coat plates. Concentrations of H84T and D133G ranged from 0.0001 to 10 μM. Data are representative of three independent experiments. (**B** and **C**) Competition ELISA for H84T binding to HA. A fixed amount (0.1 μM) of H84T was used, while the concentrations of the known BanLec ligand methyl α-D-mannopyranoside in (B) or galactose, not a BanLec ligand, in (C) were varied (0.0001-0.1 μM). Data are representative of three independent experiments. Error bars denote the standard error of the mean of technical triplicate values.

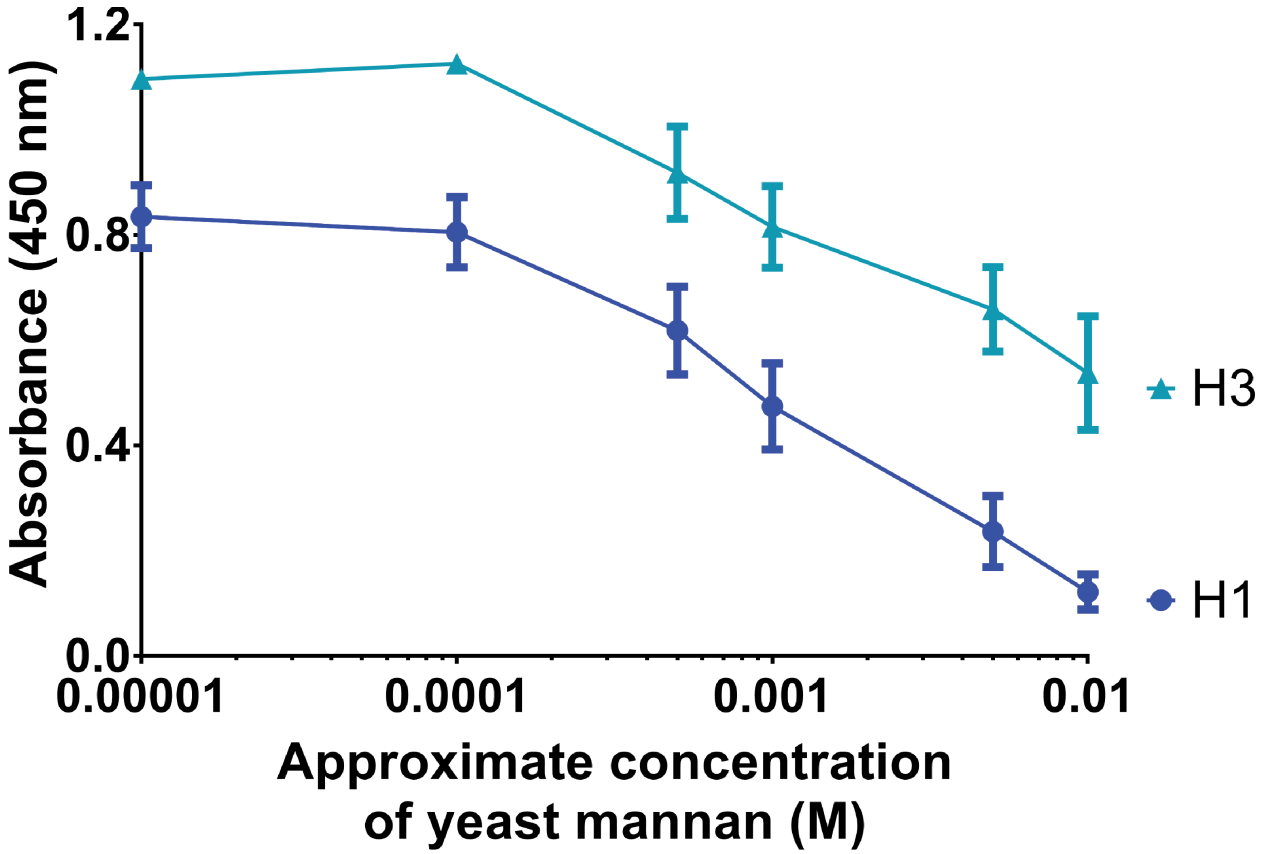

Figure 2.10 Yeast mannan inhibits H84T binding to HA.

Competition ELISA for H84T binding to HA. A fixed amount (0.1 μM) of H84T was used, while the concentrations of yeast mannan, a mannose-rich predicted BanLec ligand, were varied (0.00001-0.01 μM). Concentrations are approximate because yeast mannan is a heterogeneous mixture of molecules with different numbers of mannose residues. Error bars denote the standard error of the mean of technical triplicate values. Data are representative of three independent experiments.

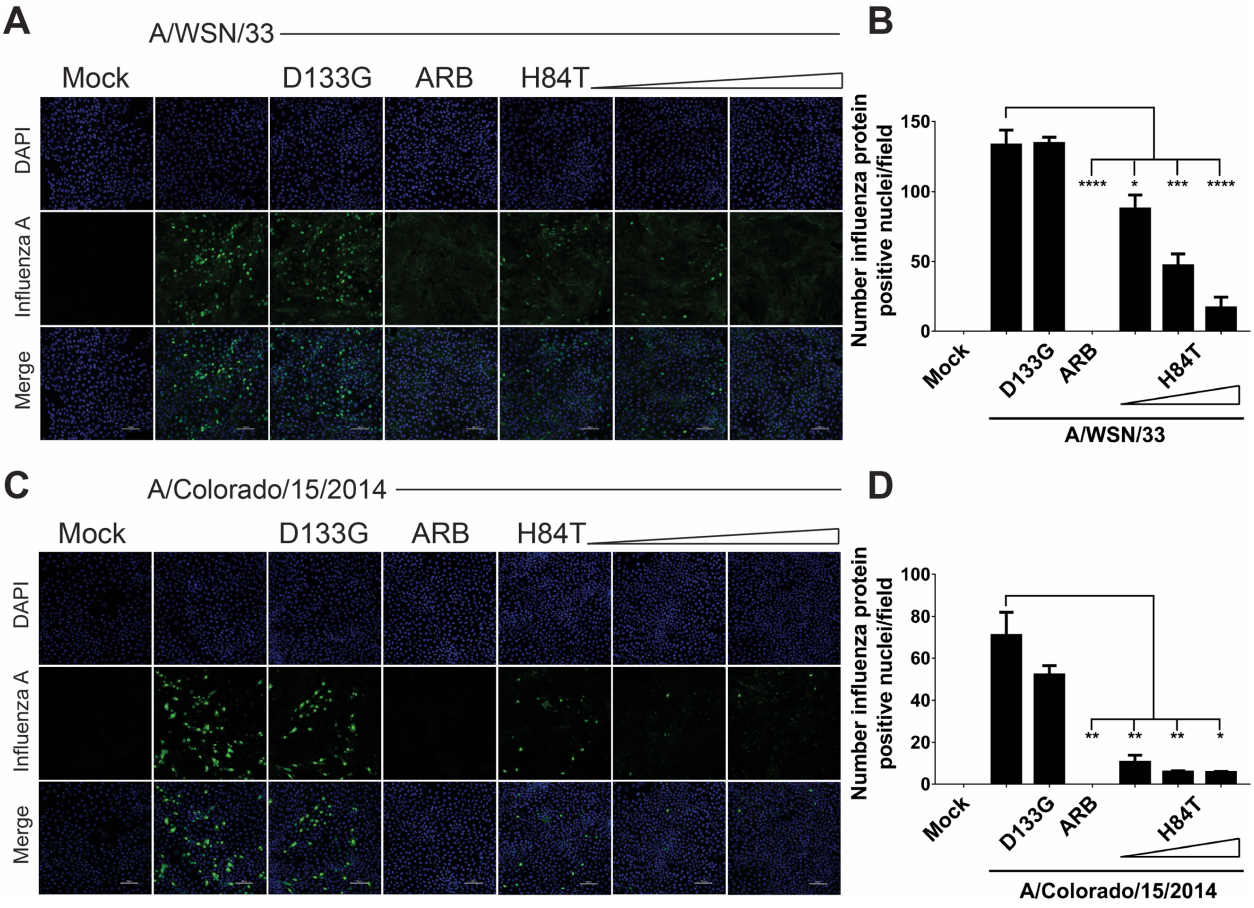

Figure 2.11 H84T prevents influenza virus protein expression in MDCK cells.

(**A** to **D**) MDCK cells were pre-treated for 1 h with H84T (0.1, 1, or 10 μM in [A]; 0.05, 0.1, or 1 μM in [C]), 10 μM D133G, or 40 μM of the fusion inhibitor arbidol (ARB) and infected with A/WSN/1933 (H1N1) (**A**) or A/Colorado/15/2014 (H3N2) (**C**) (MOI 0.5) for 5 h at 37ºC. (**A** and **C**) Representative immunofluorescent micrographs of influenza A antigen staining (green) and nuclei (blue) 5 h post-infection. Data for (A) and (C) are representative of three and four independent experiments, respectively. (**B** and **D**) Quantitation of the number of cells with influenza protein-positive nuclei per field, as assessed by a trained observer in a blinded fashion. Statistical analyses were performed by *t* test. **P* < 0.05, ***P* < 0.01, ****P* < 0.001, and *****P* < 0.0001, as compared to the infected, untreated group. Error bars denote the standard error of the mean.

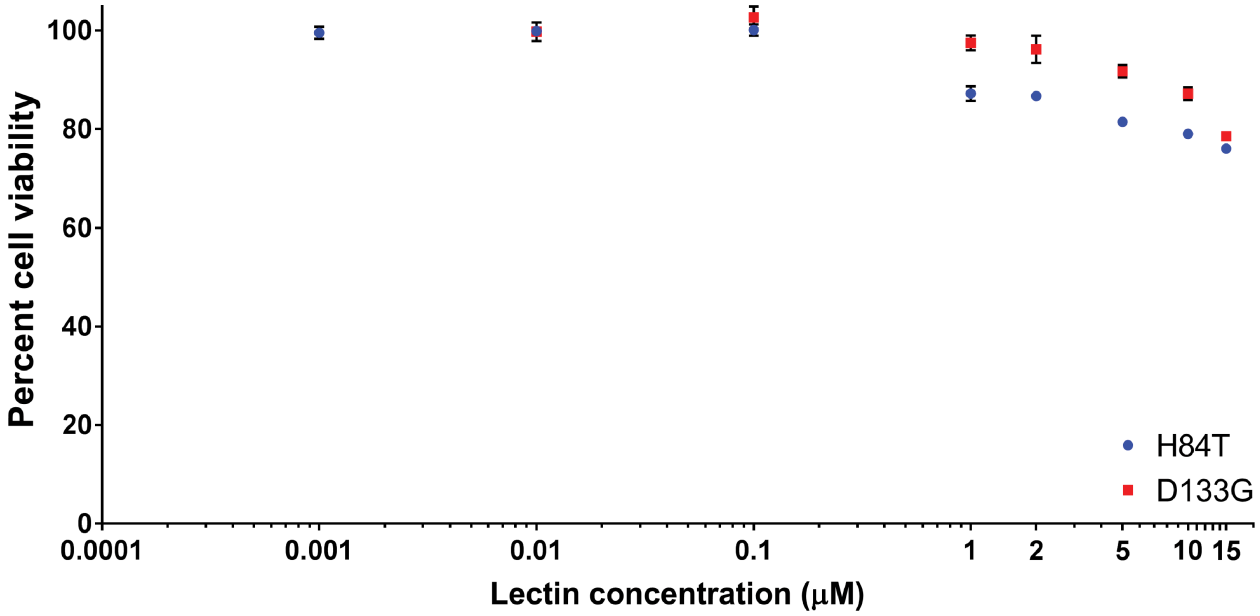

Figure 2.12 H84T is not cytotoxic to MDCK cells at IC_{50} concentrations.

Triplicate wells of MDCK cells were treated for 24 h with H84T or D133G (0.001-15 μM). Cytotoxicity was assessed by MTT assay and normalized to untreated cells. Error bars denote the standard error of the mean. Data are representative of three independent experiments.

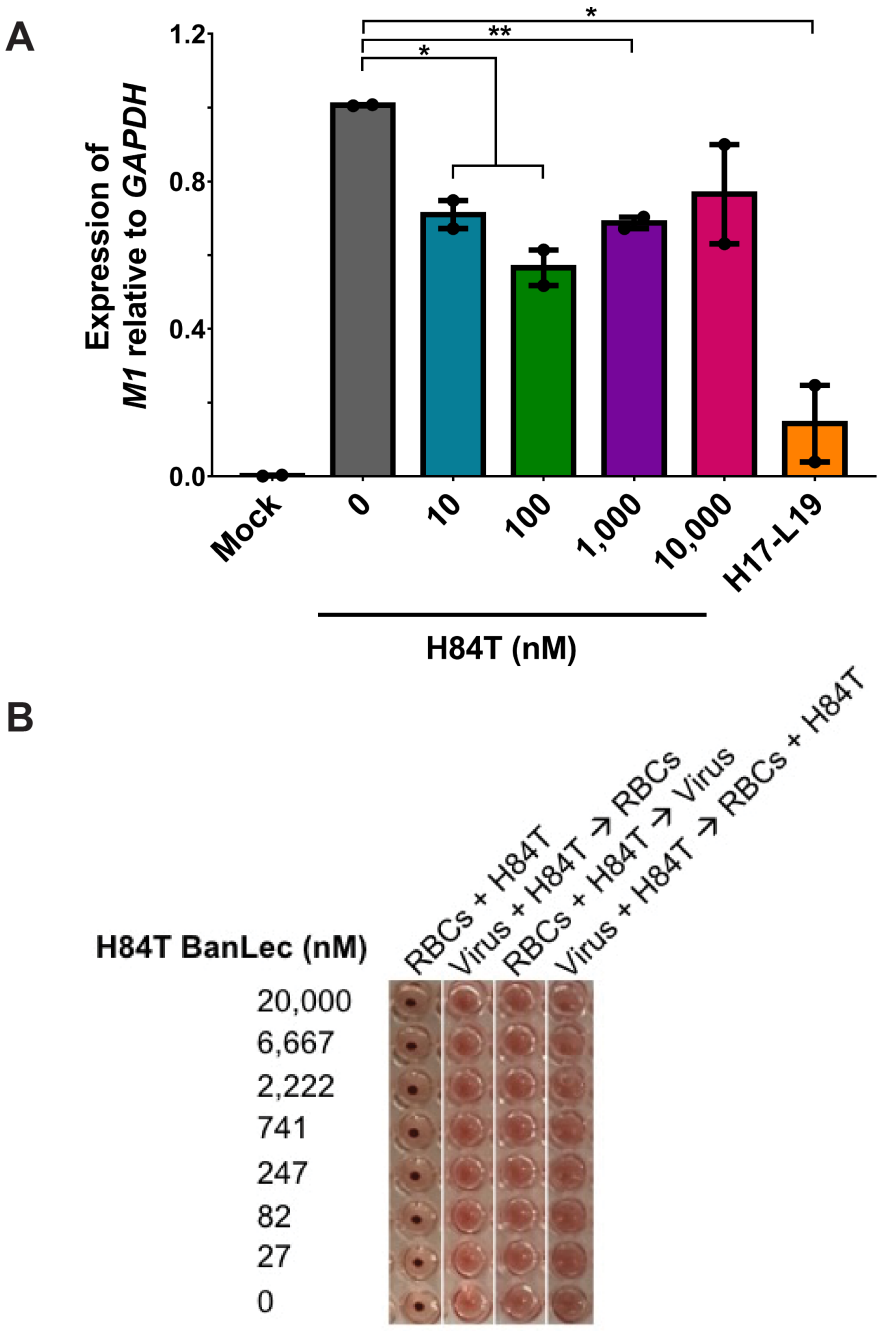

Figure 2.13 H84T minorly inhibits influenza virus attachment.

(**A**) A/WSN/1933 was incubated with 0-10,000 nM H84T for 30 min at 25ºC and the virus-H84T mixture incubated with MDCK cells for 1 h at 4ºC. Excess virus was removed and cells were collected in Trizol for RNA extraction. The relative amount of cell-associated virus was assessed by qRT-PCR using primers specific to influenza *M1*, normalized to *GAPDH* expression. The positive control for attachment inhibition is the H17-L19 monoclonal antibody against A/WSN/1933. The negative control for *M1* amplification by qRT-PCR is mock infection. Bars represent the mean values two independent experiments performed in technical duplicate, and error bars represent the standard error of the mean. Statistical significance was determined by *t*

test. *$P < 0.05$ and **$P < 0.01$, as compared to the infected, untreated group. (**B**) Binding of A/WSN/33 to cells was monitored by its ability to hemagglutinate turkey red blood cells (RBCs). H84T was pre-incubated with virus (virus + H84T → RBCs), with cells (RBCs + H84T → virus), or with both cells and virus (virus + H84T → RBCs + H84T) before hemagglutination. Data are representative of two independent experiments. Experiment in B performed by S.R.K.

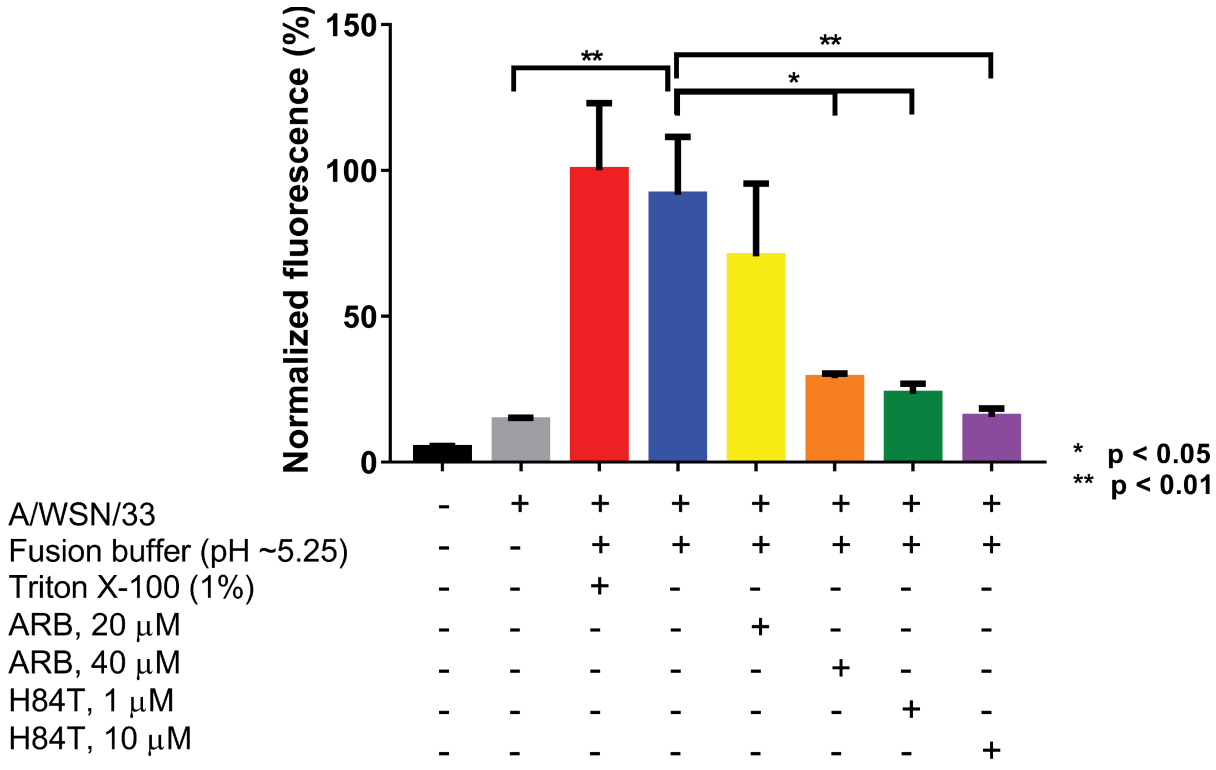

Figure 2.14 H84T inhibits influenza virus fusion.

MDCK cells were pre-treated for 1 h at 37ºC with 1 or 10 μM H84T or 20 or 40 μM of the fusion inhibitor arbidol (ARB) and incubated with octadecyl R18-labeled A/WSN/1933 for 1 h at 4ºC to allow attachment only. Excess virus was removed and virus fusion with the cell membrane was triggered at 37ºC using pH ~5.25 fusion buffer. Fluorescence dequenching of R18 was monitored on a microplate fluorometer with excitation and emission wavelengths of 560 and 590 nm, respectively. Maximal dequenching was achieved with 1% Triton X-100 set at 100%. Bars represent the mean values from duplicate wells from two independent experiments and error bars represent the standard error of the mean. Statistical analyses were performed by *t* test. *$P < 0.05$, **$P < 0.01$, comparing groups indicated by brackets.

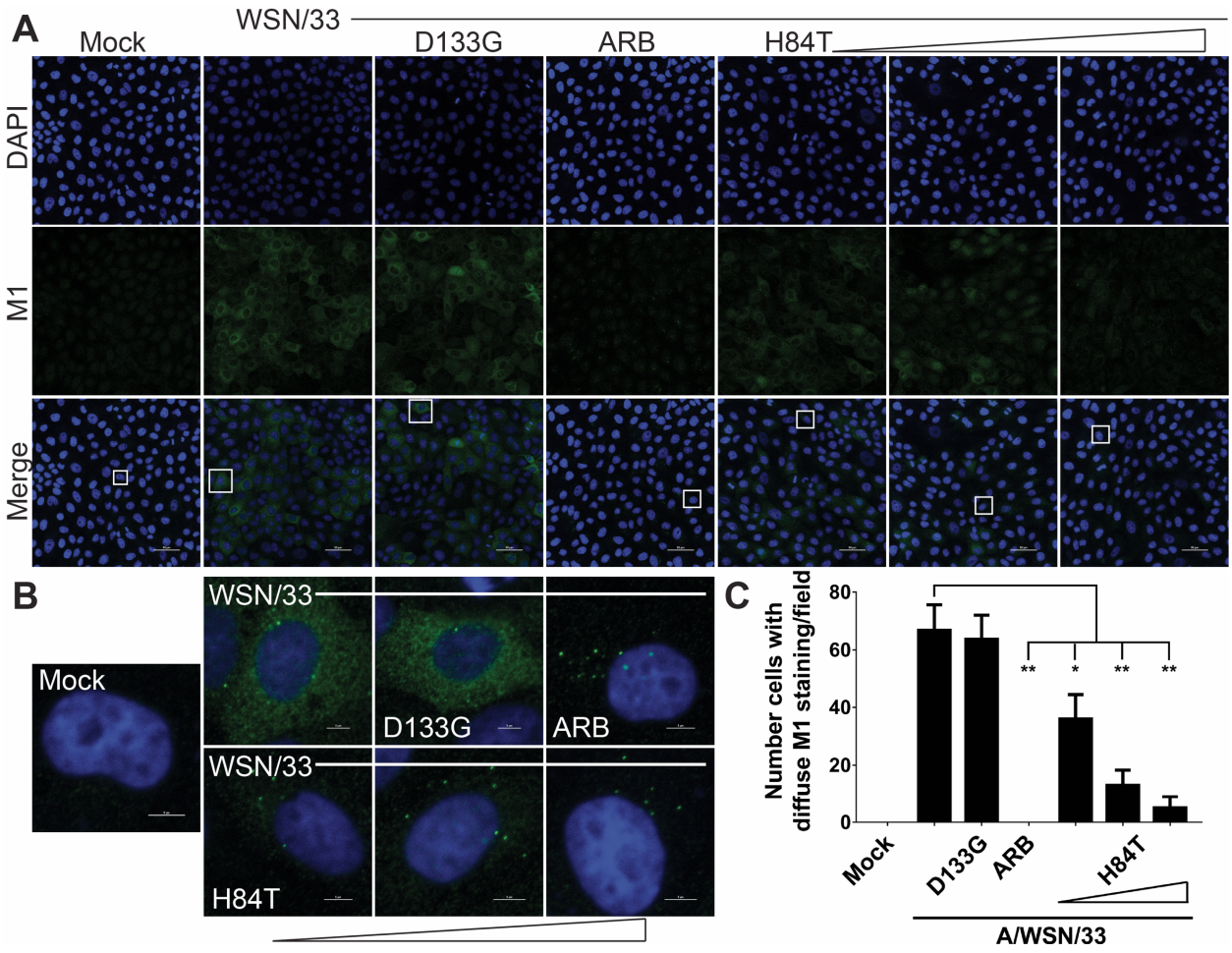

Figure 2.15 H84T reduces influenza virus uncoating.

(**A** to **C**) MDCK cells were pre-treated for 1 h with 0.1, 1, or 10 μM H84T, 10 μM D133G, or 40 μM of the fusion inhibitor arbidol (ARB) and infected with A/WSN/1933 (MOI 0.5) for 2.5 h at 37ºC. (**A**) Representative immunofluorescent micrographs of M1 antigen staining (green) and nuclei (blue) 2.5 h post-infection. (**B**) Micrographs of single cells from (A). Data for (A) and (B) are representative of fifteen independent experiments. (**C**) Quantitation of the number of cells with diffuse cytoplasmic M1 staining per field, as assessed by a trained observer in a blinded fashion. Statistical analyses were performed by *t* test. **P* < 0.05, ***P* < 0.01, and *****P* < 0.0001, as compared to the infected, untreated group. Error bars represent the standard error of the mean.

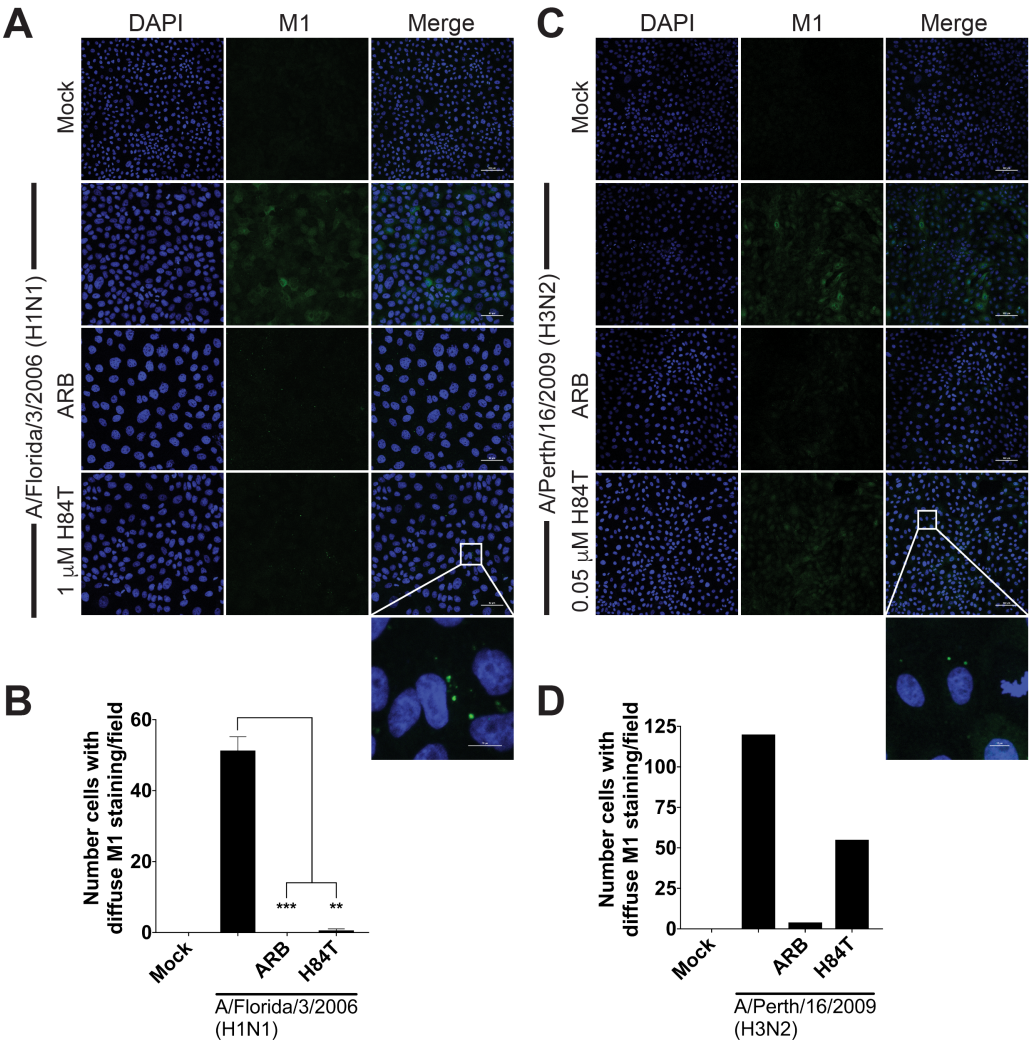

Figure 2.16 H84T reduces uncoating of multiple diverse strains of influenza.

(**A** and **B**) MDCK cells were pre-treated for 1 h with 1 (A) or 0.05 (B) μM H84T or 40 μM of the fusion inhibitor arbidol (ARB) and incubated with A/Florida/3/2006 (H1N1) (A) or A/Perth/16/2009 (H3N2) (B) (MOI 0.5) for 2.5 h at 37ºC. Immunofluorescence was visualized by confocal microscopy. (A and B) Representative immunofluorescent micrographs of M1 antigen staining (green) and nuclei (blue) 2.5 h post-infection. Data for (A) and (B) are representative of three independent experiments each. (**C** and **D**) Quantitation of the number of cells with diffuse cytoplasmic M1 staining per field. Statistical analyses were performed by *t* test. $^{**}P < 0.01$, and $^{***}P < 0.001$, as compared to the infected, untreated group. Error bars represent the standard error of the mean.

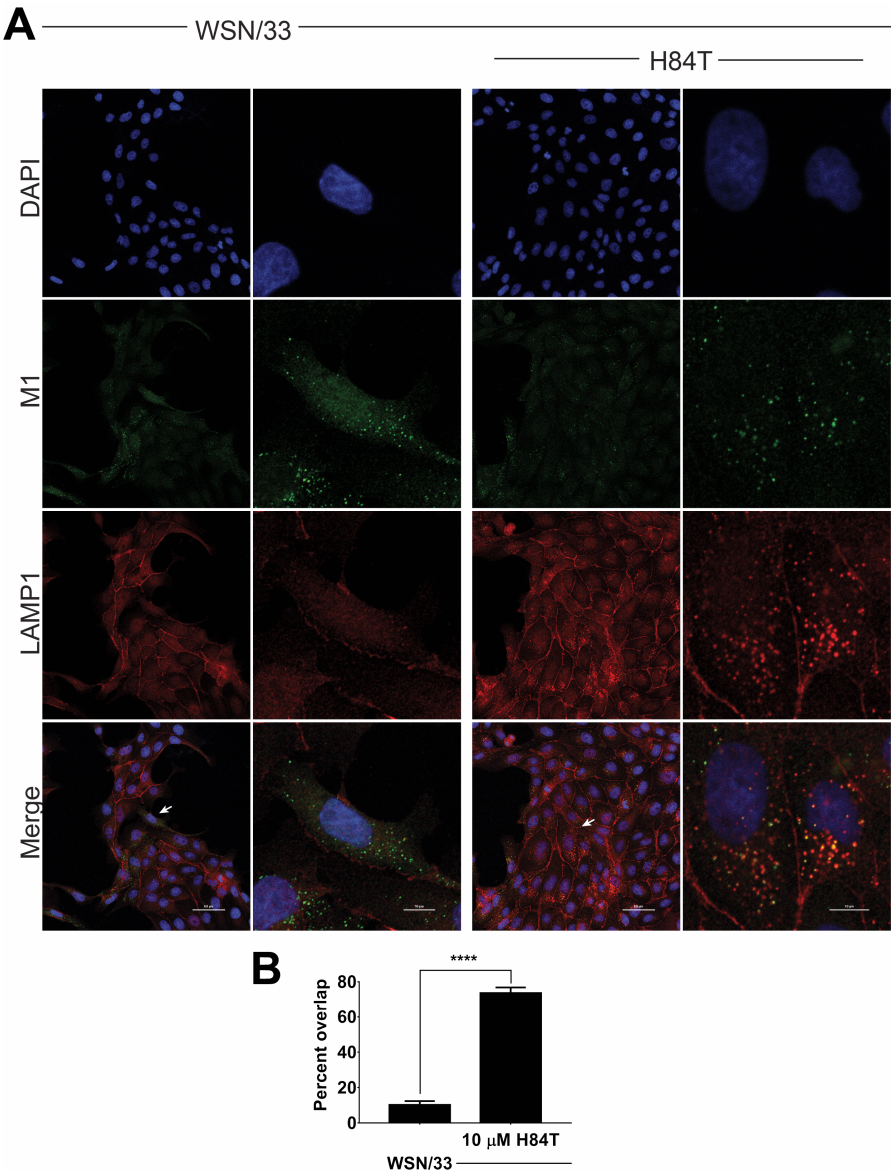

Figure 2.17 H84T restricts influenza virus to the late endosomal/lysosomal compartment.

(**A**) Representative immunofluorescent micrographs of M1 (green) and LAMP1 antigen staining (red) and nuclei (blue). Following 1 h pre-treatment with H84T (10 μM), MDCK cells were incubated with A/WSN/1933 (H1N1) at 4ºC for 1 h to allow only for attachment, excess virus was removed, treatment-containing medium was replaced, and the cells were incubated at 37ºC for an additional 3 h. The second and fourth columns are micrographs of one or two cells from the first and third columns, respectively, indicated by the arrows. Data are representative of five independent experiments. (**B**) Quantitation of the percent of M1-positive punctae that are also LAMP1-positive (percent overlap). Statistical analyses were performed by *t* test. ****$P <$ 0.0001, as compared to the infected, untreated group. Error bars represent the standard error of the mean.

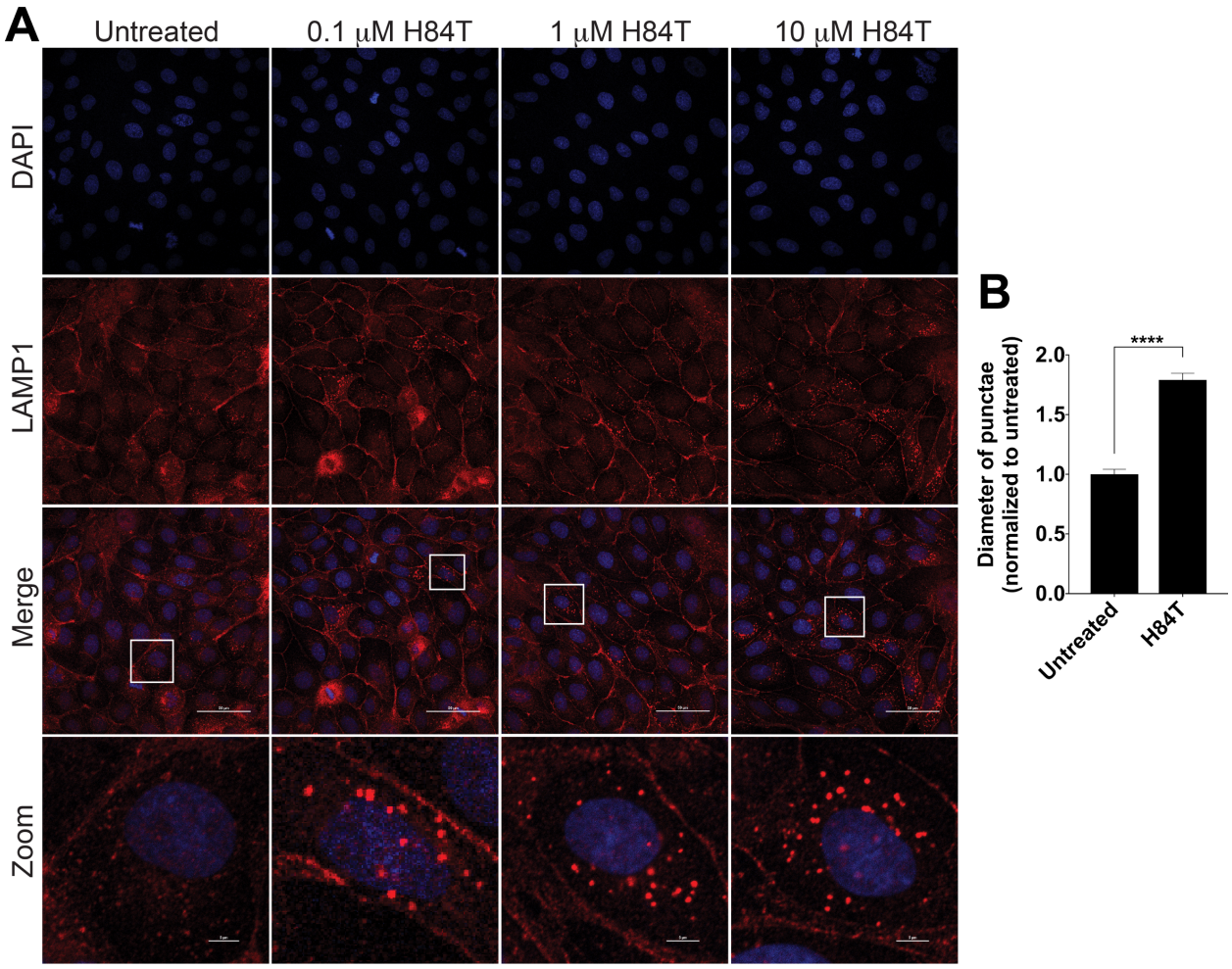

Figure 2.18 H84T treatment alone increases the number of large LAMP1-positive punctae.

(**A**) Representative immunofluorescent micrographs of LAMP1 antigen staining (red) and nuclei (blue) in MDCK cells 4 h post-treatment with 0.1, 1, or 10 μM H84T. No influenza virus was added. Immunofluorescence was performed to detect LAMP1 antigen. The bottom row (zoom) shows micrographs depicting single cells from the merged images, indicated by the boxes. Data are representative of two independent experiments. (**B**) Quantitation of the size (diameter) of punctae in the untreated versus 10 μM H84T-treated cells. Statistical analyses were performed by *t* test. ****$P < 0.0001$, as compared to the untreated group. Error bars represent the standard error of the mean.

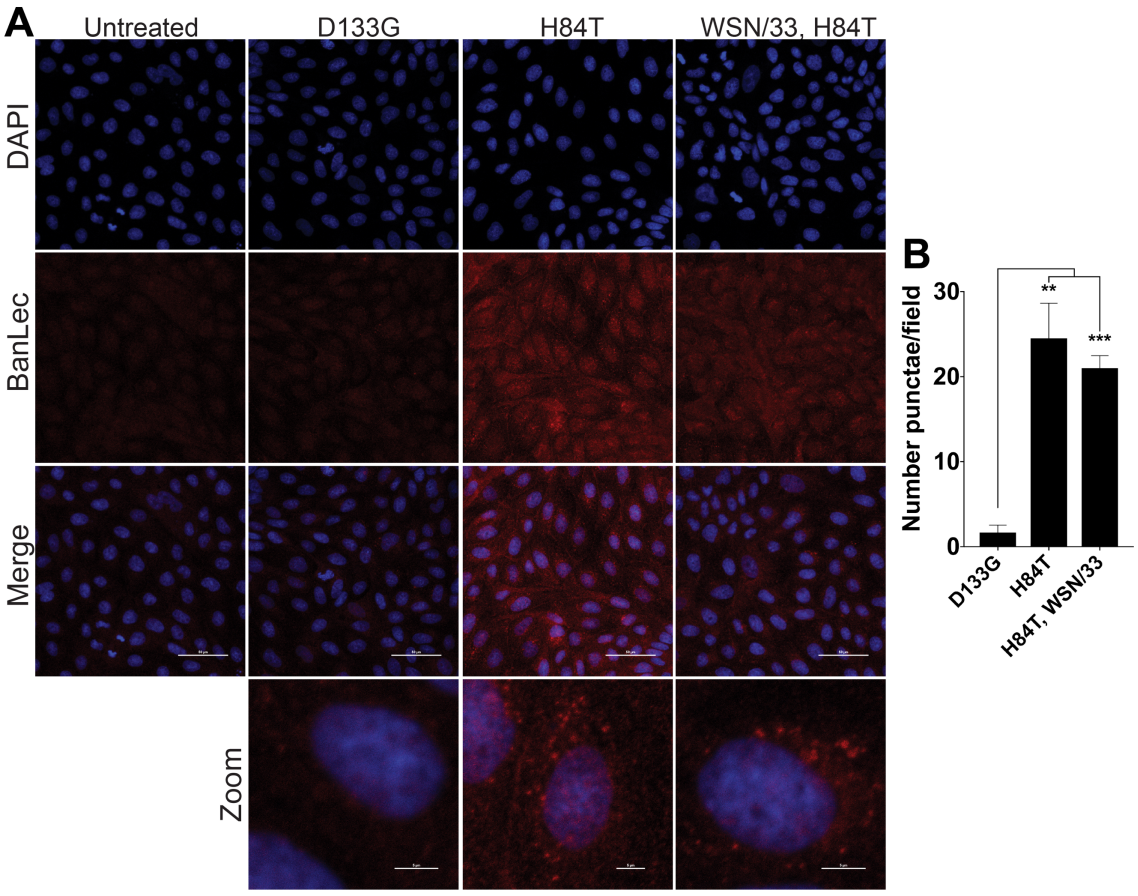

Figure 2.19 H84T but not D133G is internalized into cells.

(**A**) Representative immunofluorescent micrographs of BanLec antigen staining (red) and nuclei (blue). Following 1 h pre-treatment with D133G or H84T (10 μM), MDCK cells were incubated or mock incubated with A/WSN/1933 (H1N1) at 4ºC for 1 h to allow only for attachment, excess virus was removed, treatment-containing medium was replaced, and the cells were incubated at 37ºC for an additional 3 h. The bottom row (zoom) shows micrographs depicting single cells from the merged images, indicated by the boxes. Data are representative of two independent experiments. (**B**) Quantitation of the number of BanLec (D133G or H84T)-positive punctae per field. Statistical analyses were performed by *t* test. $^{**}P < 0.01$, $^{***}P < 0.001$, as compared to the D133G-treated group. Error bars represent the standard error of the mean.

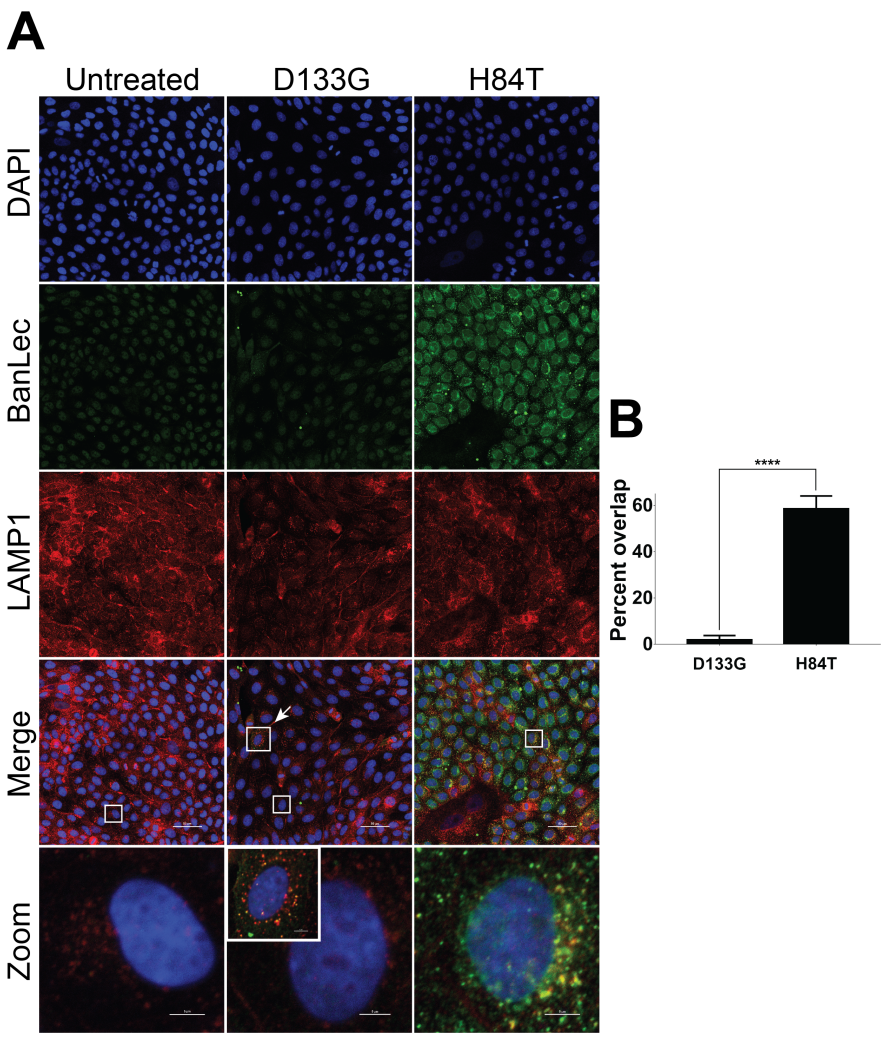

Figure 2.20 H84T is internalized into the late endosome/lysosome.

(**A**) Representative immunofluorescent micrographs of BanLec antigen staining (green), LAMP1 staining (red), and nuclei (blue). MDCK cells were incubated or mock incubated at 37ºC for 4 h with D133G or H84T (10 μM). The bottom row (zoom) shows micrographs depicting single cells from the merged images, indicated by the boxes. The cell depicted in the inset is indicated by an arrowhead. Data are representative of four independent experiments. (**B**) Quantitation of the percent of BanLec (D133G or H84T)-positive punctae that are also LAMP1-positive (percent overlap). Statistical analyses were performed by *t* test. ****$P < 0.0001$, as compared to the D133G-treated group. Error bars represent the standard error of the mean.

Table 2.1 Effect of Oseltamivir Carboxylate and H84T BanLec combination on an influenza A/California/07/2009 (H1N1)pdm09 virus infection in MDCK cells. Mean ± standard deviation from two studies.

Experiment performed by D.F.S.

Oseltamivir Carboxylate (μg/ml)	**Virus Titer (log_{10} $CCID_{50}$/ml) H84T BanLec (μg/ml)**								
	32	**10**	**3.2**	**1.0**	**0.32**	**0.1**	**0.032**	**0.01**	**0**
3.2	0	0	0	0	0	0	0	0	0
1.0	0	0	0	0	5.3 ± 0.4	5.5 ± 0.3	5.2 ± 0.2	5.7 ± 0.9	4.2 ± 0.2
0.32	0	0	0	0	4.5 ± 0.7	5.1 ± 0.8	5.7 ± 0.9	5.8 ± 0.4	5.3 ± 0.4
0.1	0	2.6 ± 0.1	3.8 ± 0.4	3.4 ± 0.5	4.3 ± 0.4	5.9 ± 0.6	6.2 ± 0.2	6.7 ± 0.5	6.8 ± 0.4
0.032	0	2.2 ± 0.2	3.4 ± 0.5	5.3 ± 0.4	4.9 ± 0.2	7.3 ± 0.4	7 ± 0.4	6.9 ± 0.2	7 ± 0.4
0.01	0	2.4 ± 0.1	4.2 ± 0.2	5.4 ± 0.1	5 ± 0	7 ± 0.4	7.2 ± 0.2	7 ± 0.4	7.4 ± 0.1
0.0032	1.7 ± 0	3.8 ± 0.4	5.8 ± 0.4	6.7 ± 0.9	6.4 ± 0.5	7.6 ± 0.1	7.3 ± 0.4	7.2 ± 0.2	7.8 ± 0.4
0	1.9 ± 0.2	4.6 ± 0.1	7.2 ± 0.2	7.2 ± 0.2	7.4 ± 0.1	6.9 ± 0.2	7.6 ± 0.1	7.4 ± 0.5	7.9 ± 0.2

Oseltamivir carboxylate EC_{90} = 0.06 μg/ml
H84T BanLec EC_{90} = 3.8 μg/ml

The shaded area indicates a possible region of synergy defined as a one-log (or greater) decrease in virus titer when compared to both individual drugs alone.

Table 2.2 Effect of Oseltamivir Carboxylate and H84T BanLec combination on an influenza A/Perth/16/2009 (H3N2) virus infection in MDCK cells. Mean ± standard deviation from two studies.

Experiment performed by D.F.S.

Oseltamivir Carboxylate (µg/ml)	**Virus Titer (log_{10} $CCID_{50}$/ml) H84T BanLec (µg/ml)**								
	32	**10**	**3.2**	**1.0**	**0.32**	**0.1**	**0.032**	**0.01**	**0**
3.2	0	0	0	0	0	0	0	0	0
1.0	0	0	0	0	0	0	1.9 ± 0.2	2.4 ± 0.1	3.8 ± 0.4
0.32	0	0	0	0	0	2.8 ± 0.4	2.6 ± 0.1	3.5 ± 0.7	4.3 ± 0.4
0.1	0	0	0	0	0	2.9 ± 0.6	2.8 ± 0.4	3.2 ± 0.2	4.3 ± 0.4
0.032	0	0	0	0	0	3.4 ± 0.5	4.2 ± 0.2	4.8 ± 0.4	5.6 ± 0.1
0.01	0	0	0	0	3.8 ± 0.4	4.4 ± 0.5	4.8 ± 0.4	4.8 ± 0.4	5.8 ± 0.4
0.0032	0	0	0	0	3.9 ± 0.6	3.8 ± 0.4	5.6 ± 0.1	5.8 ± 0.4	6.8 ± 0.4
0	1.9 ± 0.2	0	0	0	4.2 ± 0.2	5.3 ± 0.4	6.8 ± 0.4	6.9 ± 0.6	7.5 ± 0.7

Oseltamivir carboxylate EC_{90} = 0.005 µg/ml
H84T BanLec EC_{90} = 0.04 µg/ml

The shaded area indicates a possible region of synergy defined as a one-log (or greater) decrease in virus titer when compared to both individual drugs alone.

Table 2.3 Effect of Oseltamivir Carboxylate and H84T BanLec combination on an influenza A/Duck/Minnesota/1525/81 (H5N1) virus infection in MDCK cells. Mean ± standard deviation from two studies.

Experiment performed by D.F.S.

Oseltamivir Carboxylate (μg/ml)	**Virus Titer (log_{10} $CCID_{50}$/ml) H84T BanLec (μg/ml)**								
	32	**10**	**3.2**	**1.0**	**0.32**	**0.1**	**0.032**	**0.01**	**0**
3.2	0	0 ± 0	0 ± 0	0 ± 0	0 ± 0	0 ± 0	0 ± 0	0 ± 0	0 ± 0
1.0	0	2.0 ± 0.4	2.3 ± 0.4	2.8 ± 0.4	3 ± 0.7	3.1 ± 0.6	2.8 ± 0.7	2.6 ± 0.1	2.3 ± 0.4
0.32	0	2.9 ± 0.6	2.8 ± 0.4	4 ± 0.4	3.8 ± 0.4	4 ± 0.7	4.6 ± 0.1	4.4 ± 0.1	3.9 ± 0.6
0.1	3.0 ± 0.7	3.8 ± 0.4	5.9 ± 0.6	6.2 ± 0.2	6.4 ± 0.1	6.2 ± 0.2	5.8 ± 0.4	6 ± 0.4	5.8 ± 0.4
0.032	4.8 ± 0.4	5.3 ± 0.4	7.3 ± 0.4	7.5 ± 0.3	6.9 ± 0.2	7.1 ± 0.6	6.9 ± 0.8	7.6 ± 0.1	7.3 ± 0.4
0.01	4.9 ± 0.6	5.3 ± 0.6	7.2 ± 0.2	6.6 ± 0.1	7.2 ± 0.2	7 ± 0.4	7.2 ± 0.2	7.3 ± 0.4	7.8 ± 0.4
0.0032	5.8 ± 0.4	4.9 ± 0.6	7.6 ± 0.1	6.7 ± 0.5	7.1 ± 0.6	7.3 ± 0.4	7.3 ± 0.4	7.2 ± 0.7	7.3 ± 0.4
0	5.9 ± 0.6	6.4 ± 0.1	7.3 ± 0.4	7.6 ± 0.1	7.4 ± 0.1	7.3 ± 0.4	7.2 ± 0.2	7.1 ± 0.6	7.6 ± 0.1

Oseltamivir carboxylate EC_{90} = 0.17 μg/ml
H84T BanLec EC_{90} = 7.8 μg/ml

The shaded area indicates a possible region of synergy defined as a one-log (or greater) decrease in virus titer when compared to both individual drugs alone.

Table 2.4 Effect of Oseltamivir Carboxylate and H84T BanLec combination on an influenza B/Brisbane/60/2008 virus infection in MDCK cells. Mean ± standard deviation from two studies.

Experiment performed by D.F.S.

Oseltamivir Carboxylate (μg/ml)	**Virus Titer (log_{10} $CCID_{50}$/ml) H84T BanLec (μg/ml)**								
	32	**10**	**3.2**	**1.0**	**0.32**	**0.1**	**0.032**	**0.01**	**0**
3.2	0	4.6 ± 0.1	4.5 ± 0.7	4.5 ± 0.7	4.0 ± 0.7	4.5 ± 0.7	6.0 ± 0.7	5.6 ± 0.1	5.4 ± 0.5
1.0	0	4.2 ± 0.2	4.5 ± 0.7	4.8 ± 0.4	5.8 ± 0.4	5.0 ± 0.7	6.4 ± 0.5	5.5 ± 0.7	6.3 ± 0.4
0.32	3.2 ± 0.2	4.0 ± 0.4	4.9 ± 0.6	5.0 ± 0.7	6.0 ± 0.4	6.5 ± 0.7	6.8 ± 0.4	6.6 ± 0.1	7.3 ± 0.4
0.1	3.8 ± 0.4	4.3 ± 0.4	5.9 ± 0.6	6.3 ± 0.4	6.1 ± 0.6	7.0 ± 0.4	7.4 ± 0.1	7.4 ± 0.1	7.4 ± 0.1
0.032	4.0 ± 0.4	4.5 ± 0.7	6.0 ± 0.7	6.1 ± 0.6	6.8 ± 0.4	7.4 ± 0.1	7.3 ± 0.4	7.3 ± 0.4	7.6 ± 0.1
0.01	5.3 ± 0.4	4.8 ± 0.4	6.3 ± 0.4	6.2 ± 0.2	6.5 ± 0.7	7.1 ± 0.6	7.0 ± 0.4	7.2 ± 0.2	7.3 ± 0.4
0.0032	5.2 ± 0.2	4.9 ± 0.6	6.2 ± 0.2	6.4 ± 0.1	6.7 ± 0.5	7.2 ± 0.7	7.1 ± 0.6	7.0 ± 0.4	7.2 ± 0.2
0	5.6 ± 0.1	6.0 ± 0.7	6.4 ± 0.1	6.5 ± 0.3	6.6 ± 0.1	6.8 ± 0.4	6.8 ± 0.4	6.9 ± 0.6	7.4 ± 0.1

Oseltamivir carboxylate EC_{90} = 0.90 μg/ml

H84T BanLec EC_{90} = 2.1 μg/ml

The shaded area indicates a possible region of synergy defined as a one-log (or greater) decrease in virus titer when compared to both individual drugs alone.

Table 2.5 Plasma pharmacokinetics of H84T.

Experiment designed by E.L.

Dose (mg/kg)	**C_{max} (ng/ml)**	**T_{max} (hr)**	**AUC_{last} (ng*hr/ml)**	**$t_{1/2}$ (h)**	**AUC/ Dose**
5.0	110	4.5	2011	93	402
15.0	1065	4.3	14558	238	971
50.0	20435	3.5	184715	33.5	3694

Maximum concentration, C_{max} (ng/ml or ng/g)
Time at which maximum concentration occurs, T_{max} (hrs)
Area under the curve, AUC, total exposure levels (ng*hrs/ml)
Half-life, $t_{1/2}$ (hrs)

Table 2.6 Lung tissue pharmacokinetics of H84T.

Experiment designed by E.L.

Dose (mg/kg)	**C_{max} (ng/g)**	**T_{max} (hr)**	**AUC_{last} (ng*hr/g)**	**$t_{1/2}$ (h)**	**AUC/ Dose**
5.0	17160	5	460345	32	92069
15.0	60492	5	1691649	29	112777
50.0	180638	8	6183249	25	123665

Maximum concentration, C_{max} (ng/ml or ng/g)
Time at which maximum concentration occurs, T_{max} (hrs)
Area under the curve, AUC, total exposure levels (ng*hrs/ml)
Half-life, $t_{1/2}$ (hrs)